PHILOSOPHICAL TRANSACTIONS OF THE ROYAL SOCIETY A MATHEMATICAL, PHYSICAL & ENGINEERING SCIENCES

Review Lecture Electronic Aids to Night Vision

P. Schagen

Phil. Trans. R. Soc. Lond. A 1971 **269**, 233-263
doi: 10.1098/rsta.1971.0030

REVIEW LECTURE

ELECTRONIC AIDS TO NIGHT VISION

By P. SCHAGEN

Mullard Research Laboratories, Vacuum Physics Division, Redhill, Surrey

(*Delivered* 19 *March* 1970—*MS. received* 18 *June* 1970)

[Plates 4 and 5]

CONTENTS

The human eye is a very sensitive and versatile image detector, but has a number of physical limitations. The most important of these at very low light levels is the restriction in sensitivity resulting from the statistical fluctuations in the numbers of detected photons. It is shown how electronic image intensifiers can provide a fundamental improvement in this situation by capturing a larger fraction of the available photons and using these more efficiently.

The important parameters of such instruments are discussed, together with the principles of operation of their most significant component: the image intensifier tube.

This is followed by a more detailed discussion of the possible performance of night vision equipments based on different types of tube, both for direct and remote viewing applications.

1. Introduction

The spectrum of electromagnetic radiation spans more than twenty orders of magnitude in wavelength. It might, therefore, be thought surprising that the human eye is capable of using only the extremely narrow band between about 0.4 and 0.8 μm for its visual processes. However,

Vol. 269. A. 1196. (Price 19*s*. (£0.95) U.S. $2.45) 19 [Published 5 February 1971

investigation of the physical phenomena associated with the process of image formation and visual perception reveals that this wavelength interval is in fact very favourable. For example, for wavelengths above 1 mm, the diffraction limitations would give rise to a very low resolving power obtainable with a human eye of limited size, whereas below 1 mm the Earth's atmosphere is transparent only in a small number of wavelength windows, mainly situated between a few tenths of a micrometre and about 20 μm.

If to this is added the number of photons needed to carry out image formation with acceptable signal to noise ratios, it is evident that the spectral sensitivity band of the eye enables it to make the best use of the illumination provided by the Sun. This radiation peaks at about 0.6 μm and, due to the wide variation in reflectivity of various objects, can usually provide contrast ratios in the image of at least 100 to 1 for a natural scene.

An alternative evolutionary development, which in principle might have occurred, would have made use of the thermal radiation of objects at about room temperature. Admittedly this would have provided even larger numbers of available photons in the 10 μm atmospheric window, but due to the relatively small variations in the numbers of photons emitted by objects with only slightly differing apparent black-body temperature, would have resulted in a very low contrast ratio in a natural scene.

It thus appears that the human eye has evolved in such a way that its spectral sensitivity is very suitable for image perception under normal daylight conditions. The limitations to its performance are then set only by the density of detector elements on the retina and by the optical aberrations of the lens.

This limitation can be partly removed with the aid of purely optical instruments, such as a pair of binoculars or a telescope, both of which can increase the angular magnification at the expense of the total viewing angle.

At very low light levels, however, such as an outdoor scene illuminated only by starlight, the sensitivity and wavelength limitations of the eye are the most important. This is because the total number of quanta, detected by the eye at these light levels, is so small that the 'photon noise' resulting from its random fluctuations limits the minimum detectable image detail. It will be shown that under these circumstances electronic instruments, which collect a larger fraction of the available photons and use these more efficiently, can provide very significant improvements in perception over the unaided eye.

2. The perception performance of the eye as an image detector

2.1. *Acuity curves*

The performance of any image-forming device can be described with the aid of acuity curves, relating the minimum size of object detail, which can just be detected in a scene, to its brightness and contrast.

The process of detecting a difference in brightness between two adjacent object elements depends on the ability of the instrument to distinguish between the numbers of photons it receives and registers from the two elements concerned. The difference between the two numbers of photons gives rise to a 'signal'. Since the emission of photons is a random process, the statistical fluctuations in these numbers cause an associated 'noise'.

When the resulting signal : noise ratio is smaller than a critical minimum value, the instrument is incapable of detecting the object detail and its performance is accordingly photon-noise limited.

It is possible to derive a general expression, applying to all imaging devices in the photon-noise limited condition, for the minimum size and contrast of image details which can still be detected as a function of their luminance.

Consider an object element in the scene, with brightness L. The number of photons captured per second by the receiving aperture of the detector will be

$$p = Ld^2P \sin^2 \phi,$$

where d is the size of the object, P is the number of photons per second, equivalent to 1 lm (depending on the spectral distribution of the light), $\sin^2 \phi$ is the fraction captured by the receiving aperture, with $\sin^2 \phi \simeq (r/R)$ for a Lambertian diffuser, if r is the radius of the aperture and R is the distance from object to instrument.

This can also be written as

$$p = LPr^2(d/R)^2 \simeq LPr^2\alpha^2,$$

where α is the angle subtended by the object.

The introduction of suitable units for the different parameters leads to

$$p = 2.66 \times 10^{-11} LPr^2\alpha^2,$$

with L in cdm^{-2}, r in cm, and α in minutes of arc.

Consider now two adjacent elements with different luminances, L_{high} and L_{low}.

With a quantum efficiency of the detector equal to θ, and an integration time of τ seconds, the numbers of photons 'registered' by the detector during its integration time from the two adjacent elements will be:

$$p_1 = 2.66 \times 10^{-11} L_{\text{high}} \alpha^2 r^2 \tau\theta P \quad \text{and} \quad p_2 = 2.66 \times 10^{-11} L_{\text{low}} \alpha^2 r^2 \tau\theta P.$$

The 'signal' corresponding to this picture detail will thus be

$$S = p_1 - p_2 = 2.66 \times 10^{-11} (L_{\text{high}} - L_{\text{low}}) \alpha^2 r^2 \tau\theta P,$$

with an associated 'noise' of which the r.m.s. value is

$$(p_1 + p_2)^{\frac{1}{2}} = \{2.66 \times 10^{-11} (L_{\text{high}} + L_{\text{low}}) \alpha^2 r^2 \tau\theta P\}^{\frac{1}{2}}.$$

This leads to a signal : noise ratio

$$S/N = \left\{2.66 \times 10^{-11} \alpha^2 r^2 \tau\theta P \frac{(L_{\text{high}} - L_{\text{low}})^2}{(L_{\text{high}} + L_{\text{low}})}\right\}^{\frac{1}{2}}.$$

According to normal optical practice the contrast C is defined as

$$C = (L_{\text{high}} - L_{\text{low}})/(L_{\text{high}} + L_{\text{low}}),$$

and the mean luminance can be written as $L_{\text{m}} = \frac{1}{2}(L_{\text{high}} + L_{\text{low}})$.

The signal : noise ratio can thus also be expressed as

$$S/N = \{2.66 \times 10^{-11} \alpha^2 r^2 \tau\theta P L_{\text{m}} 2C^2\}^{\frac{1}{2}}.$$

This expression can be rewritten to relate more clearly the angular size α with the contrast C for the minimum detectable detail of an object, when the mean luminance is L_{m}:

$$L_{\text{m}}\alpha^2 = \frac{7.5 \times 10^{10} (S/N)^2_{\text{min}}}{D^2 \tau\theta P C^2}, \tag{1}$$

PHILOSOPHICAL TRANSACTIONS OF THE ROYAL SOCIETY A MATHEMATICAL, PHYSICAL & ENGINEERING SCIENCES

where $(S/N)_{min}$ is the minimum signal : noise ratio required for 'detection' of the object detail, and D is the effective diameter of front aperture of detector (cm).

Expression (1) is generally known as the de Vries–Rose law (Rose 1942; de Vries 1943), although in this case a few of the parameters have been defined in a slightly different way to conform with normal optical practice.

The value of the minimum signal : noise ratio required for detection depends on the type of decision which must be made, i.e. on the kind of object detail which the detector is required to resolve. For the case of suitable test objects, the value of $(S/N)_{min}$ can often be determined mathematically with the aid of probability theory (Jones 1959), by considering the number of alternative choices available, and the reliability which is required in the decision.

In the case of experiments carried out by Blackwell (1946), for instance, observers were asked to look at a circular disk, flashed on to a screen for a short period in any one of eight positions. A reliability of 50 % in the answers was required. For this situation the minimum signal : noise ratio required can be shown to be about $(S/N)_{min} = 1.5$.

When Landolt C rings are used as the test object, as in the experiments of Pirenne, Marriott and O'Doherty (1957), an observer can be asked in which one of four positions (up, down, left or right) he can see the gap in the C, with the requirement that his answers must be correct at least three out of four times. This is a four channel forced choice situation leading to about $(S/N)_{min} = 1.9$.

When determining the highest spatial frequency still resolvable with the aid of an optical system presented with black and white bar patterns the minimum signal : noise ratio required appears to be about 1.

The photon-noise limited performance, as expressed in equation (1), is not normally achievable for the smaller picture details, due to the restricted optical performance of the device. This optical performance can be described with the aid of the modulation transfer function, or m.t.f., first proposed by Schade (1948–1956), and further elaborated by Coltman (1954).

For this purpose the instrument is presented with black and white patterns of different sizes, with sinusoidal intensity cross-section. The m.t.f. of the instrument relates the modulation depth of the bar pattern in the image to the spatial frequency for 100 % contrast in the object. The performance of a complete system consisting of a number of separate components can then be described by its overall m.t.f., which is found simply by multiplying those of the individual components, provided that each of these is optically linear.

The effect of this kind of modulation transfer is an apparent reduction in the contrast C as a function of the detail size represented by the angle α.

The result on the acuity curve of a well-designed instrument is that the photon-noise limited performance which may be obtained when observing the larger object details, cannot be achieved for the smaller angles α. A typical acuity curve of such an instrument is shown in figure 1.

2.2 *The performance of the eye*

It is now possible to see how closely the eye approaches the performance of an ideal image detector with the same dimensional limitations.

In normal daylight conditions the optical performance of the eye limits its acuity. Campbell (1968) and Gubisch (1967) have recently determined the m.t.f. of the eye experimentally for different sizes of the pupil. Their results are shown in figure 2.

PHILOSOPHICAL TRANSACTIONS OF THE ROYAL SOCIETY A MATHEMATICAL, PHYSICAL & ENGINEERING SCIENCES

As the light level is reduced the number of photons registered on the retina becomes the main limitation, and the eye tries to compensate for the decreasing signal : noise ratio by various well-known means.

In the first instance the pupil dilates in order to capture more photons from the scene. The relation between the diameter of the pupil and the field luminance for an average observer, according to Walsh (1958) is shown in figure 3.

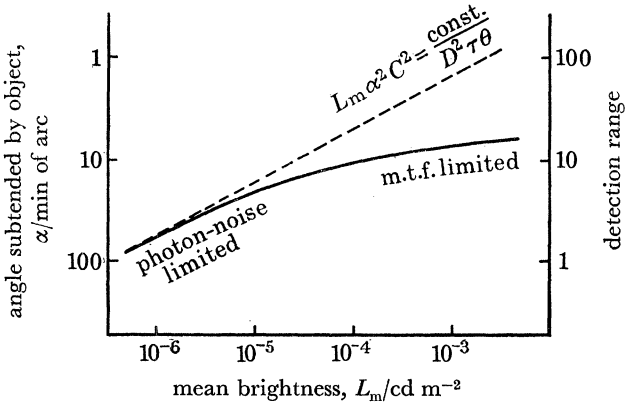

FIGURE 1. Typical performance of an image detector.

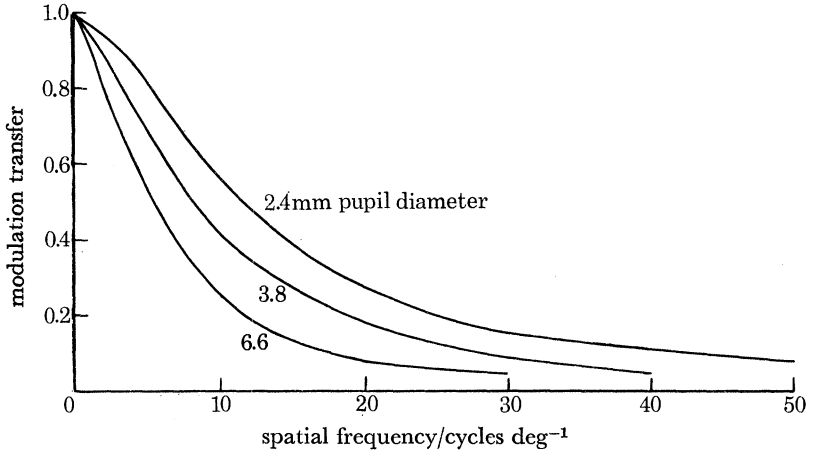

FIGURE 2. Modulation transfer functions of the human eye in white light with various artificial pupils. After Campbell & Gubisch.

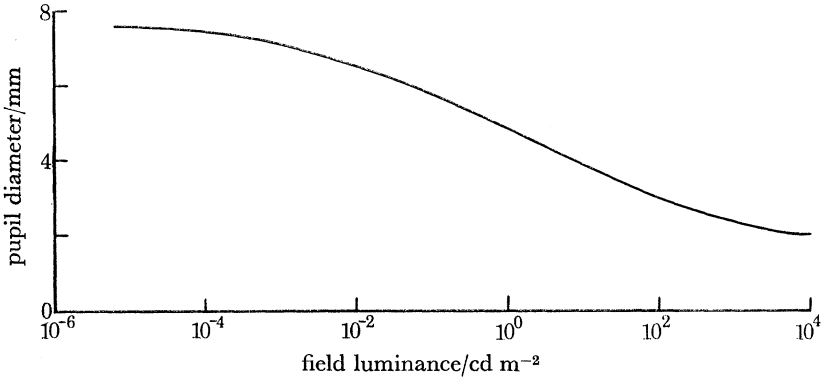

FIGURE 3. Pupil diameter of the human eye as a function of the average scene brightness.

Secondly, it may be recalled that the light-sensitive elements on the retina consist of two different groups: the 'cones', which are responsible for colour vision and operate under daylight conditions, and the 'rods' which are usually completely 'overloaded'. When the brightness of the scene drops below about 10^{-2} cd m^{-2}, the cones stop functioning and the rods slowly recover and take over. This is the well-known process of dark adaptation, which can take more than 30 min for completion.

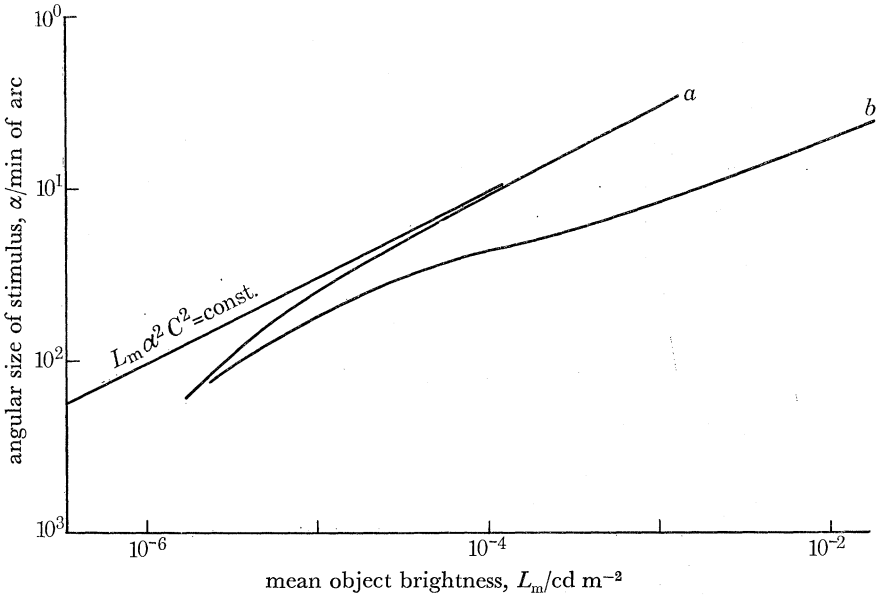

FIGURE 4. Blackwell's acuity data for 100 % contrast. Curve *a*, bright stimulus on dark background; curve *b*, dark stimulus on light background; straight line, $L_m\alpha^2C^2$ = const. (D_{eff} = 0.75 cm, τ = 0.2 s, $(S/N)_{min}$ = 1.5).

The significance of this process appears to be the fact that the network of rods and associated neurons is able to integrate the signal over larger areas of the retina, thus improving the signal: noise ratio at the expense of the ability to detect fine details. As a result, the minimum signal: noise ratio in the numbers of detected photons necessary for the perception of a particular image detail, can be maintained approximately over several orders of magnitude in retinal illumination, accompanied by a corresponding increase in size of the limiting detectable detail of a given contrast. Basically, the detective quantum efficiency of the rods does not appear to differ much from that of the cones. The pattern of connexions between rods and neurons differs, however, from that between cones and neurons, with one neuron 'integrating' the output from a number of rods and with an amount of 'cross-talk' between the neurons which depends on the illumination level. Inside the fovea, on the other hand, where only cones are to be found, the density of detector elements is much larger and each one corresponds to one neuron, thus accounting for the good limiting resolution of the eye at higher light levels, but giving rise to less spatial integration.

Thirdly, at lower scene brightness, the retina is able to integrate the signal over longer time intervals, thus improving the signal : noise ratio of the detected photons at the expense of the perceptibility of moving objects. According to Ferry-Porter's law a critical flicker frequency can be defined, which is linearly related to the logarithm of the stimulus brightness over a wide range of brightness values. The effect is still apparent at much higher light levels, such as that

of the viewing screen of a television receiver, where if the screen brightness is set excessively high an irritating 50-cycle flicker can be noticed.

For 'white' light the integration time of the fully dark-adapted eye is normally taken to be in the order of 0.2 s, decreasing to 0.1 s at a scene luminance of about 10^{-2} cd m^{-2}.

Acuity curves describing the performance of the dark-adapted or scotopic eye at low illumination levels have been carried out most extensively by Blackwell (1946), Pirenne *et al.* (1957) and their co-workers. Their results can now be compared with the performance of a photon-noise limited image detector as determined by equation (1).

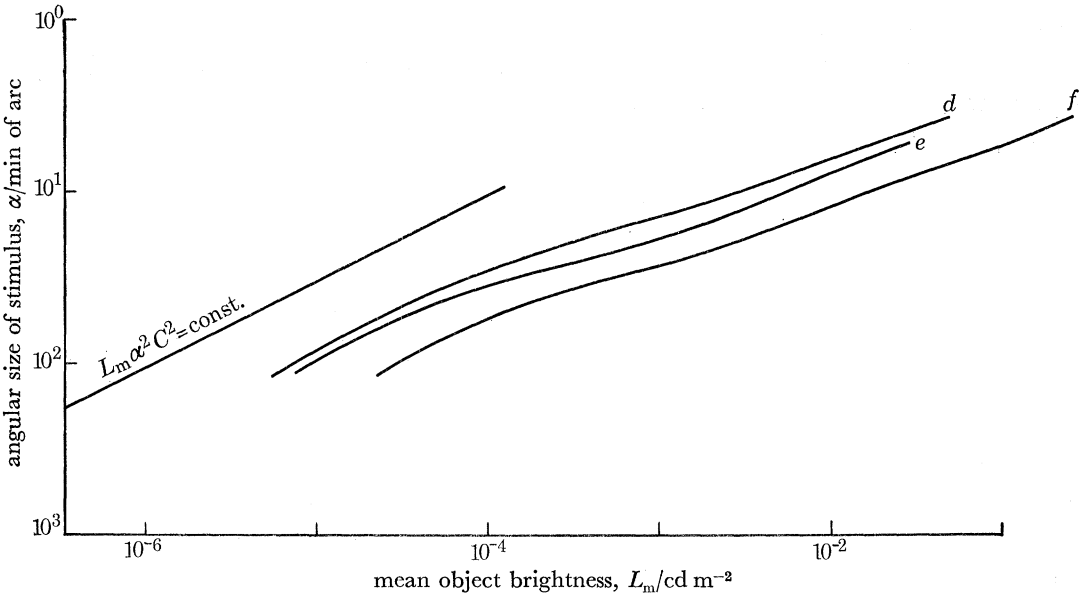

FIGURE 5. Blackwells's acuity data for lower contrast. Curve *d*, bright stimulus, $C = 0.5$; curve *e*, dark stimulus, $C = 0.5$; curve *f*, bright or dark stimulus, $C = 0.2$; straight line as figure 4.

For this purpose it must be remembered that the pupil diameter D_{eff} and the integration time τ depend on the adaptation luminance as indicated before, and that the minimum signal: noise ratio required for 'detection' depends on the type of acuity test object employed. In addition, C must be modified for the smaller size objects to take into account the optical modulation transfer of the pupil, which in turn depends on the pupil size and thus also on the adaptation luminance.

A suitable kind of acuity test in this respect would have been the type employing bar patterns as this would have made it easier to calculate the effect of the measured m.t.f. of the eye. Data of this kind for the scotopic eye have however not yet appeared in the literature.

Figure 4 shows the measured data of Blackwell for a bright stimulus on a black background (curve *a*), and for a dark stimulus on a light background (curve *b*), together with a straight light $L_m\alpha^2C^2 = \text{constant}$. L_m represents in curve *a* half the value of the stimulus

$$(L_m = \tfrac{1}{2}[L_{\text{high}} + L_{\text{low}}], \quad \text{where} \quad L_{\text{low}} = 0),$$

and in curve *b* half the value of the background. Both curves correspond to $C = 1$, where C is defined as $(L_{\text{high}} - L_{\text{low}})/(L_{\text{high}} + L_{\text{low}})$. Curve *a* shows that the retina of the fully dark-adapted eye integrates the photons in the same way as an ideal detector, according to the Vries–Rose law, with a quantum efficiency for white light in the order of about 1 %. As the integrating area

increases, however, curve *a* gradually drops below the straight line of expression (1), indicating that the integrating mechanism gradually becomes less efficient.

Curve *b* approaches curve *a* only for the largest integrating areas, and diverges quite markedly for smaller angles α. This could be due to the fact that the contribution to the noise by the background illumination for curve *b* arises from the full integrating area on the retina at that illumination level, thus giving rise to a reduced signal : noise ratio for the same signal. At the higher background illumination levels τ and D will tend to be reduced leading to an even larger divergence. In addition, at the smaller angles α the m.t.f. of the eye may begin to play a part in the arrangement corresponding to curve *b*, since the signal will in that case be spread over a larger area on the retina, leading to a reduction in contrast. A similar effect would not take place in the case of a bright stimulus on a black background, provided that the retina integrates the signal over the complete image area.

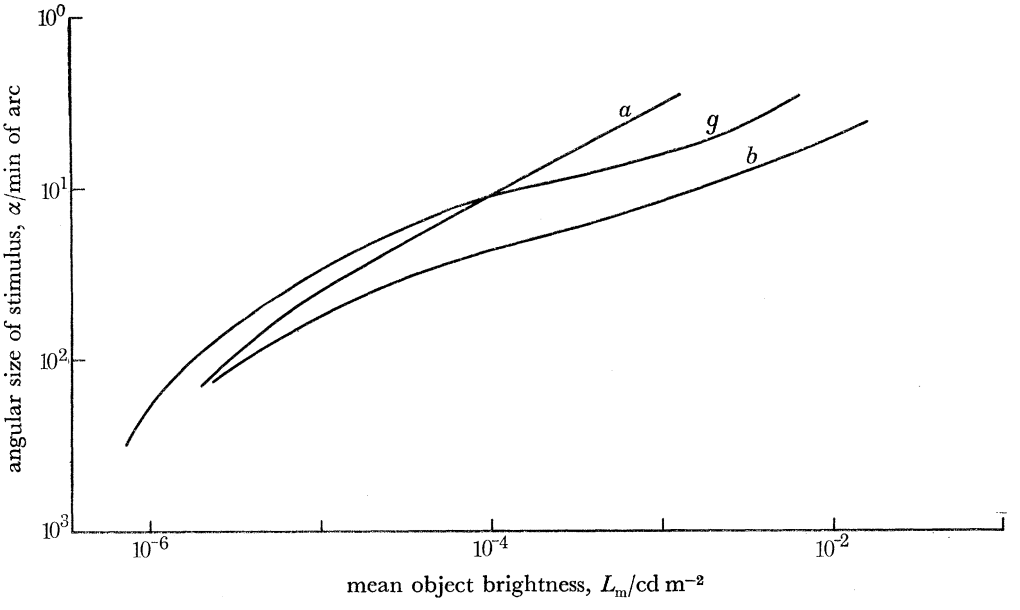

FIGURE 6. Blackwell's acuity data (curves *a* and *b*, $C = 1$) compared with Pirenne's (curve *g*).

If the contrast of the test object is reduced, the circumstances leading to curve *b* also apply increasingly to the case of a brighter stimulus on a darker background. Figure 5 shows the effect of lower contrast, with curve *d* representing the performance for $C = 0.5$ with a bright stimulus, curve *e* for $C = 0.5$ and a dark stimulus, and curve *f* representing the performance of the eye for $C = 0.2$ for both bright and dark stimuli.

The results of Pirenne's acuity measurements using black Landold C rings on a white background are shown together with Blackwell's for $C = 1$ in figure 6.

It is possible to draw the following conclusions from these experiments:

The fully dark-adapted eye integrates the detected photons on the retina very effectively over comparatively large areas, and its integrating ability decreases only slowly when the corresponding angle, subtended by the object element, approaches about 100 minutes of arc. In these conditions its performance closely resembles that of an ideal detector with an effective objective lens diameter of about 7.5 mm, an integrating time of about 0.2 s and a quantum efficiency for 'white' light of approximately 1 %. The m.t.f. of the wide open pupil begins to

restrict the resolution performance for angles smaller than about 10 minutes of arc. This limitation is somewhat reduced again at higher light levels where the diameter of the pupil is decreased and the m.t.f. is accordingly better.

2.3. *Methods of improving the performance of the eye*

The performance of the eye, as discussed above, can be improved by a number of aids.

The oldest type of instrument, intended to improve visual acuity at low light levels, is of a purely optical nature and takes the form of a pair of night glasses or a telescope. Since the front lens has a much larger diameter than the pupil of the dark-adapted eye, the instrument collects more photons from the scene. These are used to produce a correspondingly larger image on the retina. The result of this effect on the acuity curve is a shift towards smaller angles α by

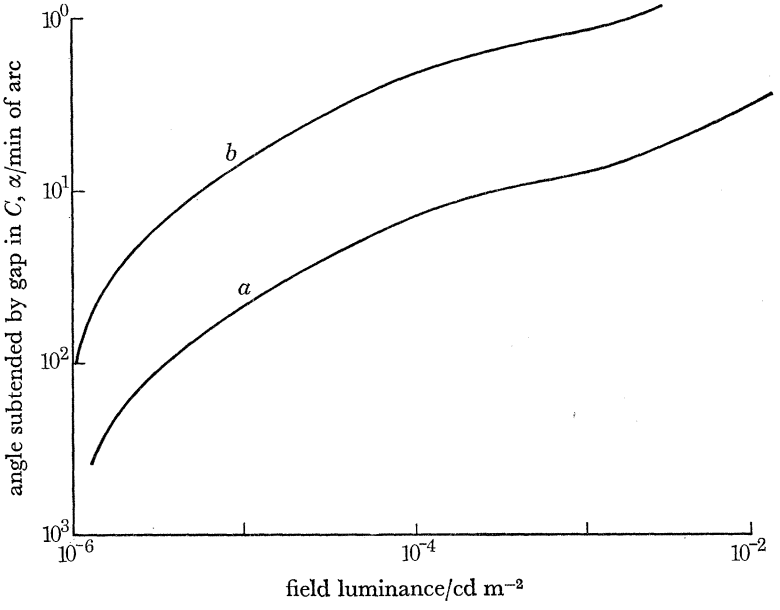

FIGURE 7. The improvement in acuity which can be achieved with a pair of nightglasses. Curve *a*, Pirenne's acuity curve for the unaided eyes; curve *b*, calculated improvement with 7×50 night glasses (70 % transmission).

a factor equal to the magnification of the instrument, and a small reduction in apparent scene brightness resulting from an unavoidable transmission loss. The exit pupil of the instrument, which is equal to the diameter of its front lens divided by its magnification factor, must exceed the geometrical size of the pupil of the dark-adapted eye in order to avoid a further reduction in apparent scene brightness. Any effect of an insufficiently good m.t.f. of the instrument will be equivalent to a reduction in contrast which becomes increasingly significant for smaller image details and causes an earlier levelling off of the acuity curve with decreasing values of α.

Figure 7 shows the improvement in acuity, which can be expected from the use of a pair of 7×50 binoculars with 70 % transmission and a sufficiently good m.t.f., when applied to Pirenne's test situation. This indicates the improvement in angular resolution, and therefore in range, which can be obtained with such an instrument. The perception improvement becomes less apparent near the absolute threshold of vision, where it can even turn into a loss as a result of the additional absorption. For this reason an instrument is needed which also shifts the acuity

curve towards lower illumination levels. This cannot be achieved by optical means alone, and has led to the development of electronic aids to night vision.

Two distinctly different types of electronic aid are possible. Both lead to 'passive' image detectors, meaning that they do not make use of additional artificial scene illumination.

The first type employs the reflected night sky radiation, received from the objects in the scene in a way similar to that of the eye, but collecting a larger fraction of the available photons and using these more efficiently. Instruments of this kind are called image intensifiers.

The other type of instrument makes use of the natural black-body radiation of the objects in the scene with the aid of thermal-image conversion. This approach is not as successful as the first in providing images with high spatial resolution in a natural scene with its low thermal contrast, and must employ a completely different detection mechanism.

The main application of thermal image detection for night vision would appear to be the addition of some of this thermal information, for instance the presence of particular 'hot spots' in the scene, to the normally intensified image.

It is beyond the scope of this paper to deal with the wide variety of ways in which thermal image conversion can be achieved. This is a subject in its own right and the further discussion will therefore be confined to image intensifiers.

Image intensifiers are either of the 'direct viewing' or of the 'remote viewing' kind. Both employ an objective optical element to collect the photons from the scene, and form an image on the photo-sensitive surface of the image tube.

In an instrument aimed at direct viewing the image tube is read out optically by presenting the observer with an intensified image on the viewing screen, which can be observed through a magnifying eye piece.

A remote viewing instrument, although it may employ similar means for an initial stage of image intensification, is similar to a standard television camera. It has an electronic read-out mechanism, which translates the charge image created by the intensified optical image, into video signals. These can be used to display a reconstituted picture on a cathode ray tube in a different location.

3. Image intensifier tubes for direct viewing

3.1. *General requirements*

The performance of an image intensifier can be expressed with the aid of acuity curves, similar to that of figure 1 for a well-designed instrument.

For the smaller picture details the m.t.f. of the instrument is the limiting factor, thus requiring the best possible optical performance of its components. The noise in the photons, detected at the photo-sensitive surface of the actual image detector, should be the only limitation when observing larger objects.

In order to achieve this photon-noise limited perception performance, two general requirements can be formulated which must be satisfied.

Each 'detected' photon, having given rise to an excited electron of one kind or another at the photo surface, must ideally result in a 'registration' on the retina of the observers's eye, over the range of screen brightnesses to be expected in practice. This requirement formulates the need for a detected-photon to viewing-photon gain in the process of image intensification. The gain must be high enough to ensure that each initial photoelectron produces so many photons at

the viewing screen, that the number absorbed by the retina will be sufficient to register an 'event'; the eye itself is not then the limiting factor.

In addition, no extraneous registrations must result from any dark current or background effects which are not related to the original image. Such additional registrations can be expressed as a constant background-equivalent illumination L_{BE} of the photosensitive surface which accordingly reduces the contrast in the image on the viewing screen to $C_{effective} = C_{screen}\, L_m/(L_m + L_{BE})$. As a result the acuity curve in figure 1 will increasingly depart from the photon-noise limited line for the low illumination levels.

At present, these two requirements can be met only if the detecting process of the photosensitive surface is of the photoemissive kind. In that case the detected photons give rise to individual photoelectrons emitted into vacuum. These may be accelerated by an external field to obtain sufficient energy to release a much larger number of photons when they strike a fluorescent material.

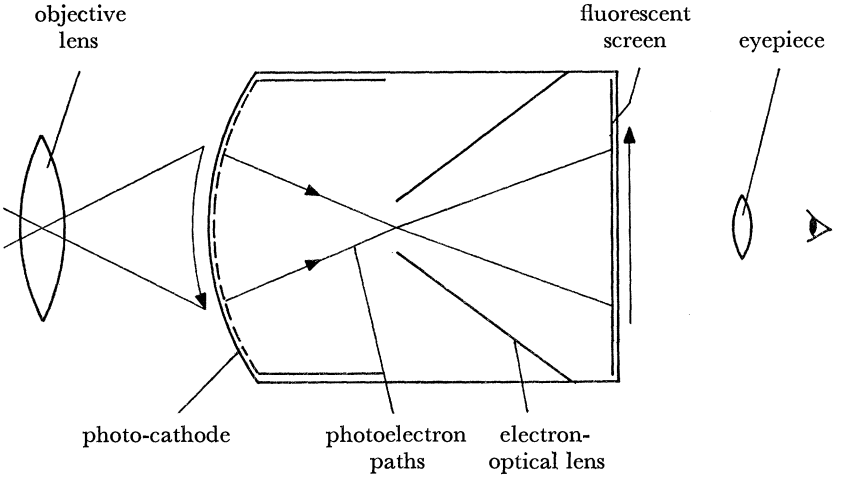

FIGURE 8. The principle of operation of a simple single-stage image intensifier tube.

Until similar effects, including a negligibly small dark-current, can be achieved inside a solid (e.g. by using avalanche multiplication), it does not seem possible to satisfy the requirements formulated above, with all-solid-state image intensifiers. For applications in the field of night vision, it thus appears that image intensifier tubes with photo-emissive cathodes are still necessary and the discussions in this paper are accordingly restricted to devices of this kind.

3.2. *Single stage tubes*

The simplest and most compact image intensifiers can be constructed by employing single-stage image intensifier tubes. Figure 8 illustrates the principle of operation of a simple tube of this kind.

An optical image of the scene is focused on the photocathode of the tube with the aid of an objective lens. Photoelectrons are emitted from the surface of the cathode in proportion to the intensity of the incident illumination. An electron-optical lens system inside the vacuum tube accelerates and focuses the electrons emitted from a small element of the photocathode onto a corresponding element of the fluorescent phosphor screen, where each electron releases a large number of photons, thus creating the intensified output image.

Modern image tubes are provided with a photocathode consisting of a compound of antimony and the alkali metals Na, K and Cs, suitably prepared to obtain maximum sensitivity at the red end of the spectrum. A typical spectral response curve of such a so-called S-25 photocathode is shown in figure 9. At present this type of cathode makes the best use of the light from the night sky in the absence of moon and clouds. The spectral distribution of starlight during an average night is illustrated in figure 10.

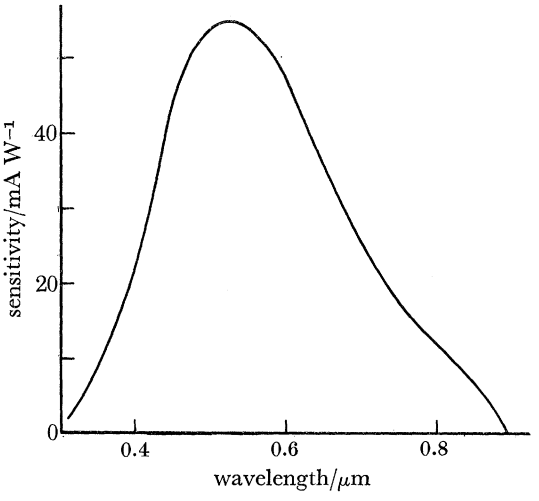

FIGURE 9. Spectral sensitivity of a typical photocathode of the S-25 type.

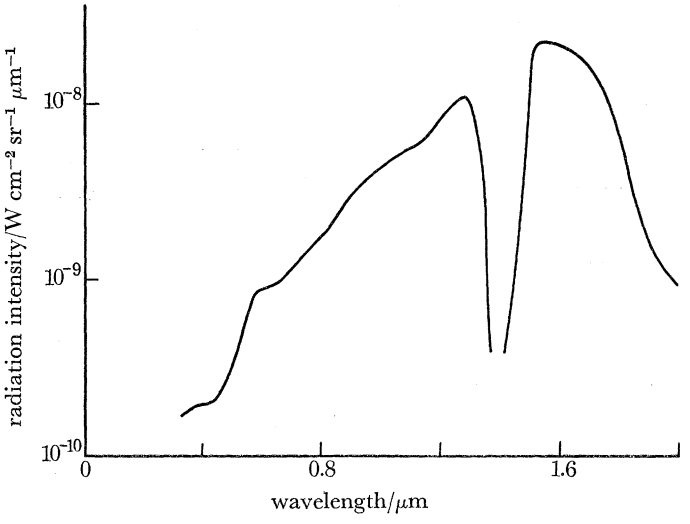

FIGURE 10. Typical distribution of radiation in the night sky.

These curves imply that a further extension of photocathode sensitivity into the infrared would be desirable. In view of the high reflectivity of green vegetation for near infrared light, this would also improve the contrast for natural scenery (Richards 1969). During recent years promising results in this respect are beginning to emerge from research on photoemission from semiconducting compounds of the GaAs type (Schagen & Turnbull 1969).

Most image intensifier tubes employ an electrostatic focusing and inverting lens derived from the original concentric sphere approach (Schagen, Bruining & Francken 1952), which enabled the

designer to lay down a few initial requirements with respect to image magnification and resolution performance. Experimental modifications of this first design model, usually with the aid of large scale models, led to the final tube design. Recent advances in the use of computers to aid the electron-optical design of these tubes (Stark, Lamport & Woodhead 1969) have made these experimental optimization procedures superfluous. Computer programs have been formulated which require only input data on the shape of the electrodes, the spectral response of the photocathode and the spectral distribution of the input radiation.

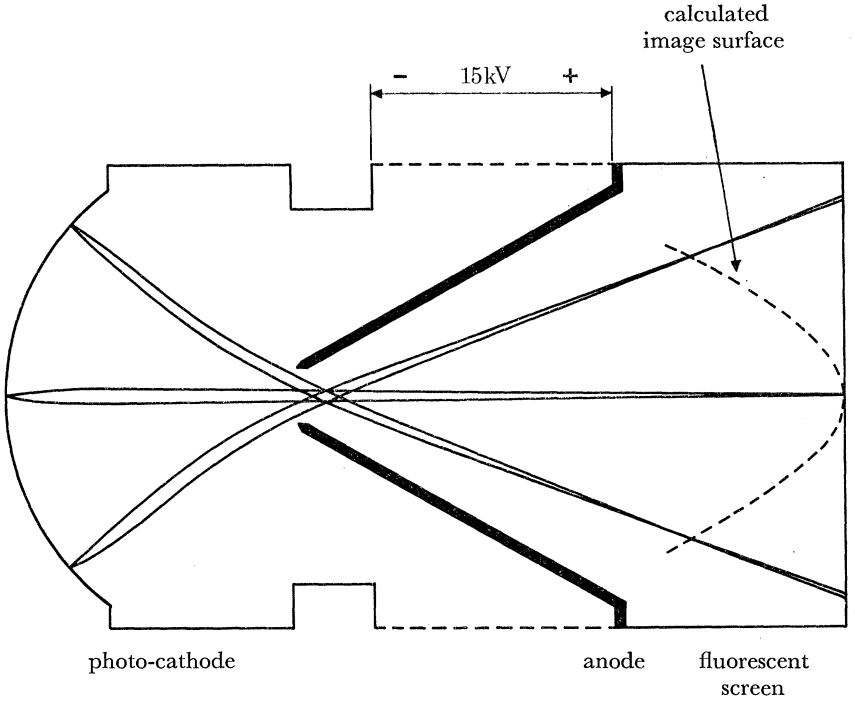

FIGURE 11. Illustration of electron trajectories in a typical image tube obtained with the aid of a computer.

Employing these data, the computer calculates the field, the electron trajectories, the point spread function on the screen of a bunch of electrons leaving a point on the photocathode, and the resulting electron-optical modulation transfer function. By combining this m.t.f. with that of the relevant phosphor screen, it is possible to predict the overall resolution performance of any particular image tube, without the need for experiments.

Figure 11 shows a few electron paths in a typical image tube, as traced with the aid of the computer data. In figure 12 an m.t.f., thus calculated, is compared with the measurements carried out on the actual tube.

This tube design procedure has also made it possible to determine the critical dimensional tolerances in the final tube manufacture. The result has been a smaller spread in characteristics, leading to image tubes with a better average performance.

It has been shown in practice that instruments employing a single-stage image intensifier tube can obtain a perception gain over the unaided eye, which under starlight conditions approaches very closely the theoretical limits indicated in the next section. This perception gain can be maintained over an even wider range of scene illumination levels by applying a certain amount of variable electron-optical image magnification inside the image tube (Woodhead, Taylor & Schagen 1963–4).

3.3. *Multi-stage tubes*

The main disadvantages of the single stage tube approach are that it requires a fully dark-adapted observer in order to optimize the perception gain, and that it is in general not feasible to obtain a screen brightness which is completely adequate for a high speed of detection and recognition of objects in a starlit scene.

For this reason the technique of employing more than one stage of image intensification has been employed. The initial idea to cascade several stages of image intensification dates back to the thirties (Barthelemy & Zeitline 1936), but the first practical tube was probably designed and built by Schaffernicht in Germany during the war (Krisek & Vand 1946). The main disadvantage of the original approach was the attempt to incorporate all the stages into one envelope. This led to serious manufacturing difficulties in preparing multiple cathodes and to severe picture distortion in all-electrostatic tubes. Figure 13 shows the schematic arrangement of an early image tube of this type.

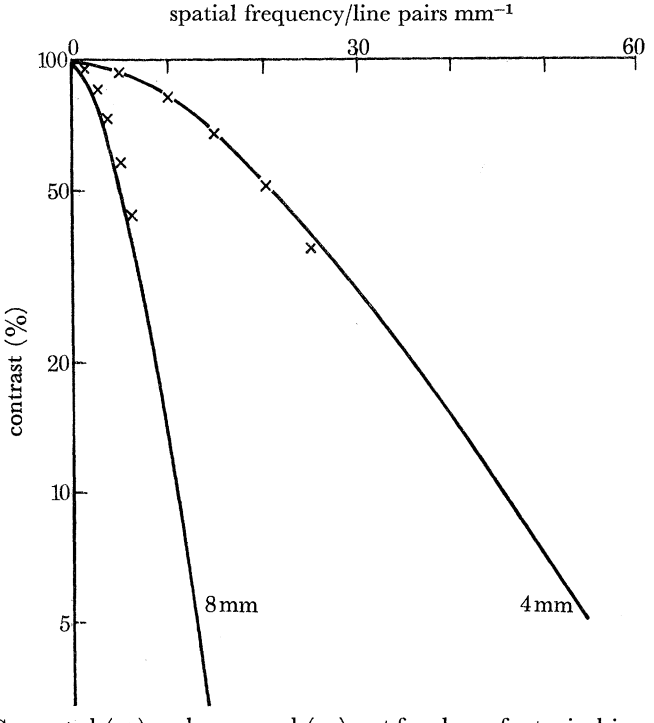

FIGURE 12. Computed (×) and measured (—) m.t.f. values of a typical image tube 4 mm and 8 mm off axis on the screen.

In an alternative approach, tubes were made with a number of secondary emission multiplication stages (Sternglass 1955), illustrated in figure 14.

Photoelectrons, emitted by the photocathode, are accelerated and focused by coaxial electric and magnetic fields on to one side of a thin membrane coated on the other side with a suitable secondary electron emitting material. A larger number of secondary electrons is emitted from the rear of the membrane, and these are again accelerated and focused on the next dynode. After a number of intensification stages of this kind, a final image is produced on the viewing screen. Very high brightness gains have been achieved in this way, but the picture contrast is seriously affected by a number of fast primary electrons penetrating the films

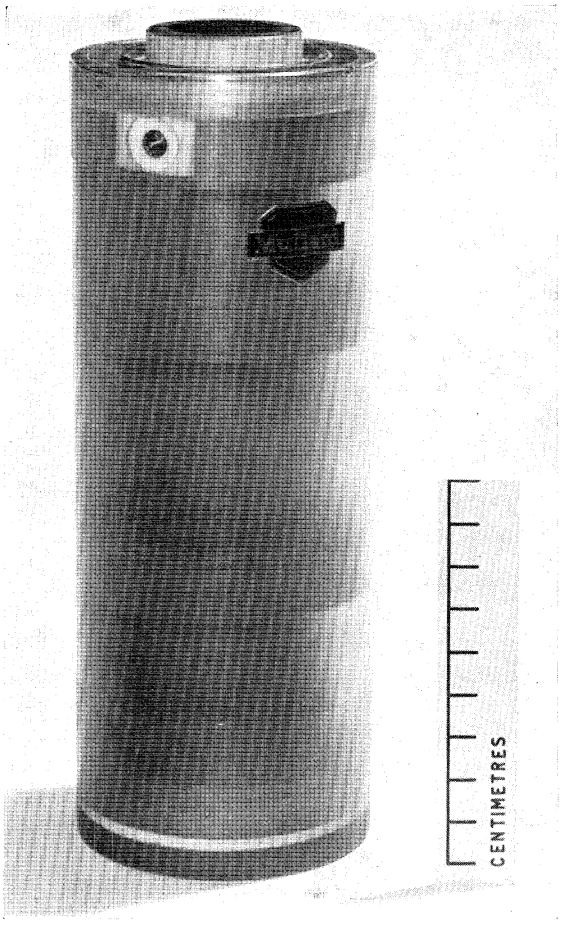

FIGURE 16. Photograph of stack of three image tube molecules with fibre-optic coupling and integral power supply unit (XX 1060).

FIGURE 22. Photograph of the image on the viewing screen of an experimental channel image intensifier tube.

(*Facing p.* 246)

PHILOSOPHICAL TRANSACTIONS OF THE ROYAL SOCIETY A MATHEMATICAL, PHYSICAL & ENGINEERING SCIENCES

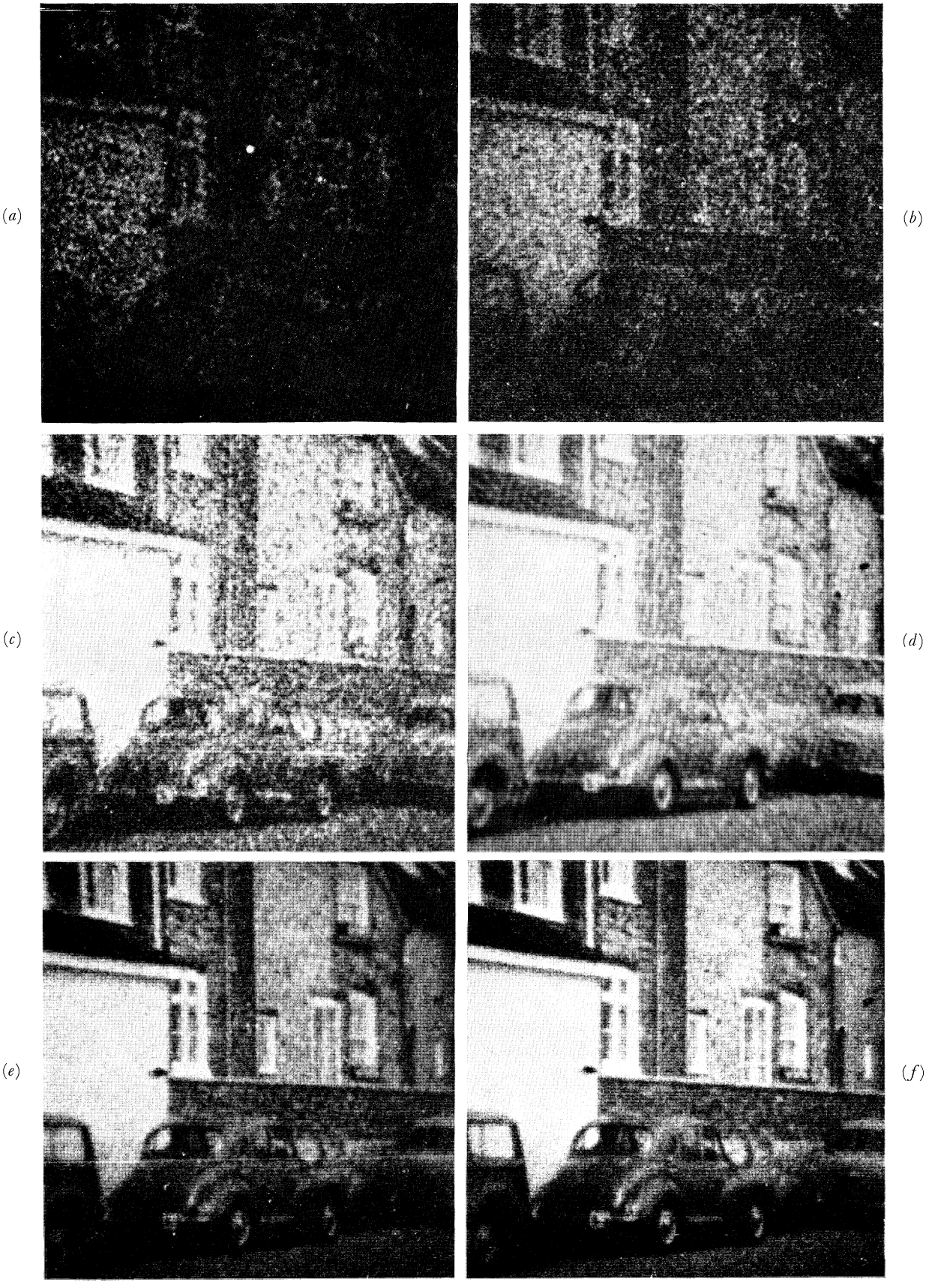

FIGURE 18. Photograph of image detail on screen of XX 1060, corresponding to different scene illumination levels, with an exposure time of 0.2 s. (*a*) 0.03 mlx (very dark sky, no moon), (*b*) 0.1 mlx, (*c*) 0.3 mlx, (*d*) 1 mlx (approx. starlight: no cloud, no moon), (*e*) 2 mlx, (*f*) 50 mlx (approx. full moon).

PHILOSOPHICAL TRANSACTIONS OF THE ROYAL SOCIETY A MATHEMATICAL, PHYSICAL & ENGINEERING SCIENCES

completely. As a result of the combined electrostatic and magnetic focusing, it is also difficult to optimize the picture quality sufficiently except in ideal laboratory conditions.

All these problems are avoided in a somewhat modified multistage approach. In this case two, and preferably three, single-stage image intensifier tube modules are stacked in cascade, using fibre-optic coupling between the output screen of one module and the photocathode of the next, as illustrated in figure 15.

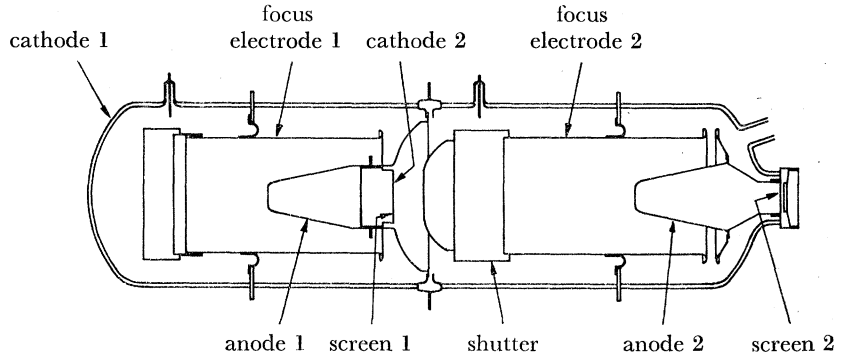

FIGURE 13. Simplified drawing of an early 2-stage image intensifier tube.

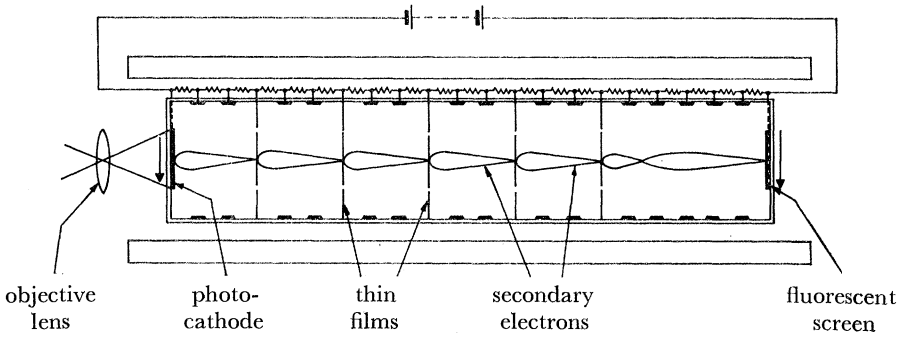

FIGURE 14. Diagram of a through-secondary-electron-multiplier tube.

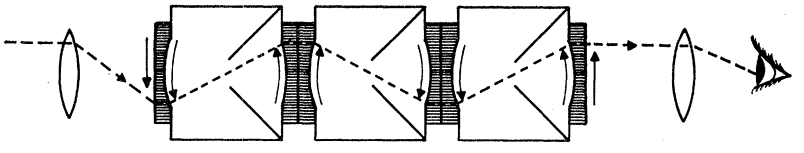

FIGURE 15. Schematic diagram of cascaded image tubes.

Stacks of fibre-optically coupled image intensifier tubes of this kind have recently left the area of strict government classification. They are now commercially available, either as individual building bricks, or as stacks of three modules encapsulated complete with a miniaturized wrap-around high voltage supply unit, as shown in the photograph of figure 16, plate 4. A stack of this kind only requires an additional miniature dry battery and oscillator, taking up no more space than a few cubic centimetres, in order to provide a completely self-contained image intensifier unit, with a brightness gain in the order of 50 000.

A typical modulation transfer function of such a stack is shown in figure 17. Figure 18, plate 5, consists of a few photographs of the image on the viewing screen for different input illumination levels and an exposure time of 0.2 s. They clearly show the scintillations corresponding to individual photons.

Due to their good performance, relatively small size, low weight, and ease of operation, these tubes have for the first time resulted in the large-scale practical application of image intensification with a high brightness gain.

However, when compared with a single-stage tube the multi-stage approach has some inherent disadvantages. These are the somewhat lower picture quality for equal photocathode and screen size, due to the cumulative effect of the modulation transfer in each of the modules, and the inevitable increase in size, weight and cost of the instrument. Also the combined effect of the six curved fibre-optic windows in a stack of three modules causes a marked decrease in brightness towards the edges of the screen. In order to keep this brightness variation within tolerable limits, it is necessary to accept a certain amount of pincushion distortion in the picture (Emberson & Long 1969).

The significance of the high brightness gain has nevertheless made this approach the preferred one for all those applications where the disadvantages noted are not prohibitive.

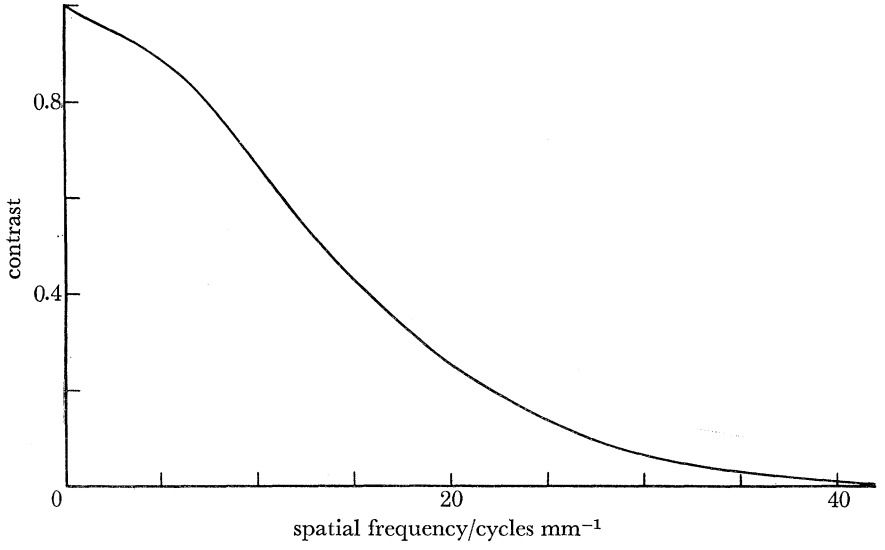

FIGURE 17. Typical modulation transfer function of a stack of three cascaded image intensifier modules (XX 1060).

3.4. *Channel tubes*

A more recent method of obtaining high brightness gain, while attempting to avoid the disadvantages of the cascaded stack, employs the principle of channel electron multiplication inside a single-stage image intensifier tube (Manley, Guest & Holmshaw 1969). This principle is based on an old idea by Farnsworth (1930), and was independently brought to practical realization in Russia (Oshchepkov, Skvortsov, Osanov & Siprikov 1960), the U.S.A. (Goodrich & Wiley 1962) and Great Britain (Adams & Manley 1965). A device based on this principle is illustrated in figure 19 where a single channel is shown, usually consisting of a glass which has sufficient electronic conduction, or of a material which is coated inside with such a glass. A potential gradient is provided along the wall of the channel. Electrons entering the channel at the cathode side, and hitting the wall, will release secondary electrons. These are drawn farther into the channel under the influence of the accelerating field, and strike the opposite wall at a higher potential, thus releasing further secondaries. This process is repeated several times, with the result that each electron entering the channel can give rise to a bunch of

electrons emerging from the other side. The electron gain depends on the ratio of length to diameter of the channel, the potential applied, and the secondary emission coefficient of the wall material. Gain values of up to about 10^8 can be obtained in practice from single channels of this kind, before space charge distorts the field and causes pulse saturation.

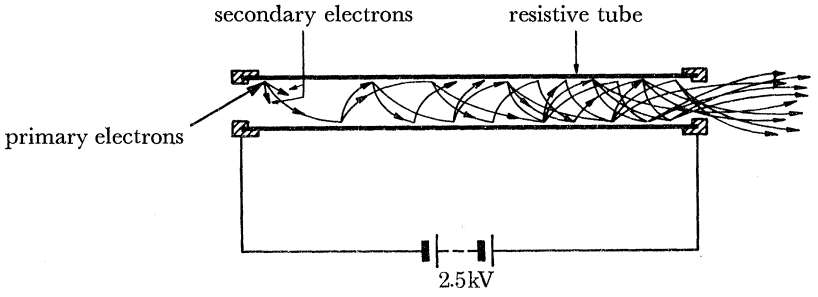

FIGURE 19. Illustration of the principle of channel electron multiplication.

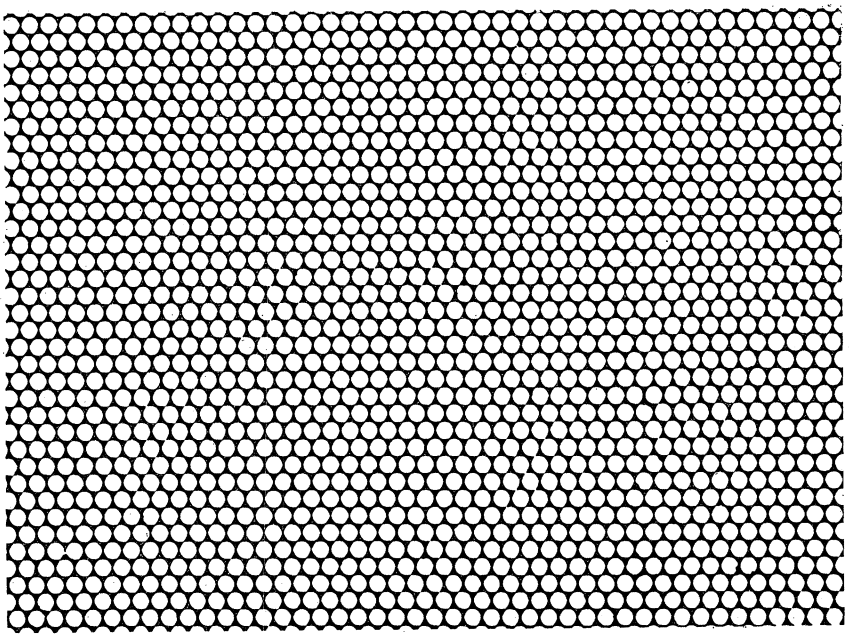

FIGURE 20. Photograph of a channel matrix as used in a channel electron multiplier tube.

The multiplication properties depend only on the ratio of length to diameter and not on the actual dimensions. Channels can therefore be made very small and stacked together with a large number of other channels to form a channel matrix or channel plate, as illustrated in figure 20. Such a channel plate can be placed between a photocathode and a fluorescent screen to form a channel electron multiplier tube. In a tube of this kind the photoelectrons are focused on to the channel plate, either with the aid of an electron-optical lens or by means of close proximity.

The corresponding electron pulses, emerging from the other side of the channel plate, are drawn across an accelerating electric field towards the fluorescent viewing screen nearby, where they cause scintillations.

As indicated schematically in figure 21, an image intensifier tube of this kind can be made in the form of a thin wafer (proximity tube), which for a direct viewing instrument needs an

optical inverter element, made for instance of optical fibres. Alternatively, the necessary image inversion can be achieved electron-optically inside the tube. This method has also advantages from the point of view of tube manufacture.

In either case the result is a combination of the small size of a single-stage image intensifier tube, with a very high brightness gain. An additional advantage is that the gain can be readily adjusted by varying the potential across the channel plate, to provide the most advantageous viewing conditions for a wide range of scene illumination levels.

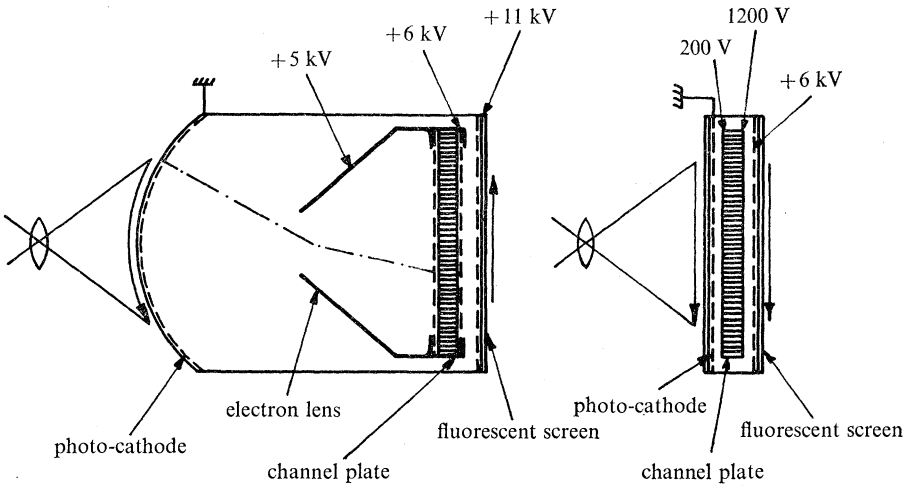

FIGURE 21. Two possible applications of the channel electron multiplication principle in an image tube.

Disadvantages of this type of image intensifier tube are the loss of photoelectrons striking the channel plate without producing an electron pulse, and the unfavourable statistical nature of the secondary emission multiplication process employed. The latter is due to the fact that the electron pulses result from a number of multiplication stages, each with a comparatively low value of the secondary emission coefficient. This leads to a quasi-exponential pulse height distribution with a noise factor, which is about twice as large as that for the more nearly Gaussian distribution of a cascaded stack of conventional image tubes. As has been pointed out in §4.3, it is not yet clear how an observer's retina–brain combination reacts to pictorial information presented in this way. Present indications are that the few very bright pulses are somewhat disturbing, although initial acuity measurements do not appear to confirm a significant loss of information.

The less favourable pulse height distribution of a channel tube can to some extent be offset as a result of the high electron gain of the channel plate. This allows the use of phosphors having lower efficiency but exhibiting a more favourable decay time than that of a P. 20 phosphor, normally used in a multi-stage tube to provide maximum brightness gain.

More pulse integration can thus be achieved to smooth out some of the increased noise. The perception performance in the photon-noise limited condition can thus be very similar to that of the conventional image intensifier tubes, although at the expense of a somewhat reduced ability to observe fast movement. The most suitable compromise between these two effects still needs to be determined in conjunction with the properties of available phosphors.

A further advantage of the channel multiplication principle is that the output current of individual channels, and thus the corresponding screen brightness, is limited by the standing current along the walls of each channel. This provides a very useful high-light limiting effect, which prevents bright light sources in the scene from completely obliterating the remainder of the picture.

A photograph taken from the screen of an experimental channel image intensifier tube is shown in figure 22, plate 4.

Tubes of this kind are at present in the development phase and further improvements are still being explored. It is therefore too early to assess their final potential compared with the multi-stage approach.

4. The most important parameters of an image intensifier for direct viewing

4.1. *Parameters which determine the basic performance limitations*

The fundamental limitation of an image intensifier equipment with regard to photon-noise is again given by expression (1). In this expression the significant parameters of the instrument must now be taken into account. If an image tube is used with a photocathode sensitivity of η amperes per lumen of night-sky radiation, the product θP in expression (1) is about $6.28 \times 10^{18} \eta$ electrons per lumen. Expression (1) thus reduces to

$$L_m \alpha^2 C^2 = \frac{1.2 \times 10^{-8} (S/N)^2_{\min}}{D^2 \tau \eta}. \tag{2}$$

If α is replaced by $57.3 \times 60\, s/R$, where s is the size of object (cm) and R is its distance or range (cm), expression (2) is transformed into

$$R = 3.14 \times 10^7 \frac{sCD}{(S/N)_{\min}} (L_m \tau \eta)^{\frac{1}{2}}. \tag{3}$$

Expressions (2) and (3) thus define the basic perception performance of the instrument, as determined by the noise in the detected photons. They also indicate the way in which this performance can be improved. The diameter of the objective lens should be chosen to be as large as possible, in order to obtain the smallest values of $L_m \alpha^2$ for a given contrast. This is one of the important factors to be considered when designing an instrument, because of its obvious implications regarding the overall size and weight of the instrument.

Also, the integration time of the instrument should be made as long as possible whenever this parameter can be controlled in a particular application. The limit in this respect must be the condition that essential information about moving objects in the scene should not be unduly sacrificed.

Taking into account the optical performance of the individual components the overall m.t.f. of the instrument can be calculated, which results in an apparent reduction in the object contrast C as a function of the angle α subtended by the object in the scene. The apparent values of C, so determined, can be substituted in expression (2), accordingly increasing the values of $L_m \alpha^2$, and thus limiting the angle α which can be observed at the higher values of the scene brightness L_m. The performance is then m.t.f. limited.

If the m.t.f. of the objective lens is much better than that of the image tube (as will normally be the case), the minimum angular resolution α in the scene will be linearly proportional to the focal length of that lens for these high brightness levels.

PHILOSOPHICAL TRANSACTIONS OF THE ROYAL SOCIETY A MATHEMATICAL, PHYSICAL & ENGINEERING SCIENCES

4.2. *The brightness of the scintillations*

In §3.1 a general requirement was formulated, which stated that each photon detected at the photocathode of the image tube should ideally result in a registration on the retina of the observer's eye. This requires a minimum electron-to-photon gain in the tube to produce scintillations which are sufficiently bright if the observer is dark-adapted, and to an even higher gain requirement if he is not.

The former can just be achieved with the aid of a single-stage image intensifier tube, provided that the eye-piece magnifies the image enough to supply the eye with a sufficiently large fraction of the photons produced in the scintillations on the viewing screen.

The higher gains can only be achieved by employing further means of brightness amplification, as in a multi-stage tube or a channel tube.

There is, however, a potential disadvantage in providing an excessively high photon gain. This results from the possible loss of picture coherence due to the disturbing effect of the scintillations, particularly at very low light levels.

Little is known about the behaviour of the eye under these conditions. There is some evidence from the experiments of Coltman & Anderson (1960), that the eye is still capable of integrating bright scintillations which are clearly recognizable individually. This would appear to indicate that an excessively high photon gain causes mainly annoyance, but no real perception loss.

Kühl, Geurts & Overhagen's experiments (1969) suggest that an optimum photon gain can be established for any particular viewing condition, which makes it possible to combine the optimum improvement in perception with the minimum disturbance caused by the scintillations. In this respect a variable photon gain, which can be adjusted by the operator for optimum comfort of viewing, seems very desirable. As indicated in §3.4, this can easily be achieved with a channel tube.

Even less is known about the effect of scintillations with a quasi exponential pulse-height distribution, like that of the channel tube.

Further experimental investigations of the perception performance of the eye when presented with 'scintillating' pictures are therefore desirable, in order to determine the optimum conditions for presenting the eye with pictorial information of this kind.

4.3. *Brightness gain*

The brightness of the viewing screen is one of the most important parameters in practical applications.

It is linearly proportional to the photon gain of the tube, and inversely proportional to the square of the *f*-number of the objective lens employed, as well as to the square of the electron optical magnification of the tube.

Although at very low screen brightness the electron-to-photon gain of the tube may be high enough to satisfy the requirement formulated in §3.1, it can take an observer a very long time to detect and recognize the significant objects in the scene, even if he is fully dark adapted.

This difficulty disappears at a higher screen brightness, and for this reason brightness gain in itself is a very important factor in the perception improvement which image intensification can provide when viewing starlit scenes, although it is difficult to express the significance of the speed and ease of recognition in quantitative terms.

PHILOSOPHICAL TRANSACTIONS OF THE ROYAL SOCIETY A MATHEMATICAL, PHYSICAL & ENGINEERING SCIENCES

A possible disadvantage of an excessively high brightness gain may in some applications be the loss of dark adaptation, which, if only in one eye, can cause some discomfort. This effect can be reduced by inserting a red filter between the observer and the viewing screen.

4.4. *Overall viewing angle*

The field of view of the instrument is determined by the ratio of the focal length of the objective lens and the useful diameter of the photocathode of the image tube.

The requirement in this respect depends of course on the application, but it is clear that the smaller the overall angle of view which can still be acceptable, the better can be the angular resolution of the instrument for the same size of photocathode, and therefore the larger its range for a high scene brightness, where it is m.t.f. limited.

A smaller viewing angle also enables the use of a lens with a larger diameter and the same f number in conjunction with the same size of tube, thus leading to a larger range also at the lower light levels, where the performance is photon-noise limited.

It is possible to trade screen brightness against angular resolution to a limited extent by varying the electron-optical magnification. This could be very desirable in a single-stage tube (Woodhead *et al.* 1963–4).

4.5. *Table of significant parameters*

Table 1 lists a few of the significant equipment parameters discussed above, expressed as a function of the relevant characteristics of tube and optical elements.

TABLE 1

image tube	brightness gain of image tube	$\dfrac{\theta G_p}{m^2}$
	photon-noise limited resolution element on photo-cathode (sensitivity 200 μA lm^{-1}, $\tau = 0.2$ s), in centimetres	$\Delta = \dfrac{5\times 10^{-6} f_0 (S/N)_{\min}}{DC(L_m)^{\frac{1}{2}}}$
instrument	brightness gain of instrument (scene-to-screen)	$\dfrac{\theta G_p D^2}{4m^2 f_0^2}$
	total angle of view of instrument	2 arc tan $d/2f_0$
	overall angular magnification of instrument	$(f_0/f_e)\,m$
	perception gain over the fully dark-adapted unaided eye in the photon-limited condition	$\dfrac{\theta}{\theta_{eye}}\left(\dfrac{D_{eff}}{0.75}\right)^2$

where θ is the quantum-efficiency of photocathode, G_p is the number of photons produced on the viewing screen per released primary photo-electron, m is the electron-optical magnification in image tube, D is the effective diameter of objective lens (cm), f_0 is the focal length of objective lens (cm), $(S/N)_{\min}$ is the minimum signal-to-noise ratio required for 'detection' of the relevant object detail, C is the contrast between object and adjacent element, L_m is the mean luminance of object and adjacent element (cd m^{-2}), d is the useful diameter of photocathode (cm), f_e is the focal length of eye piece (cm), and θ_{eye} is the quantum efficiency of retina for the radiation employed ($\theta_{eye} \sim 0.01$ for 'white' light).

5. INSTRUMENTS FOR REMOTE VIEWING

5.1. *General considerations*

The important criteria associated with television pick-up at starlight illumination levels are basically the same as those encountered in the case of direct viewing. The two factors of photon noise and modulation transfer will set the ultimate limits to the performance of the camera chain.

Additional problems, however, are created in this case by the need to translate the optical image into a pattern of electrical charges on the storage target of the pick-up tube, and to

obtain the corresponding video signal by reading this charge image out with the aid of a scanning electron beam. This process generates additional noise which may swamp the actual picture signal if the signal is not sufficiently large. In that case it may require a read-out mechanism for the scanning beam of a more complicated kind. It can also lead to serious picture lag when observing moving objects, resulting from inadequate charge removal in the scanning process.

These difficulties can only be completely avoided if a sufficiently large amount of image intensification takes place at an initial stage, preceding the formation of the charge image.

In this final section some low light level camera-tube approaches, which have given the best over-all performance to date, will be briefly discussed.

Provided that the additional problems of the television approach can be avoided, this kind of picture formation offers some important advantages.

The first one of these is peculiar to any television application, in that it makes it possible to separate the viewer from the camera and allows multiple read-out.

Secondly, video signals are very amenable to signal processing. This leads to the possibility of enhancing picture contrast by means of γ correction or black-level manipulation. It also creates the opportunity, at least in principle, to vary the integration time as required to obtain optimum perception gain for different viewing conditions, by modifying the scanning speeds.

A further advantage is that the final picture, observed by the viewer, need not necessarily be presented on a very small phosphor screen requiring a magnifying lens. It appears to be much more pleasant to view the screen of a moderately small cathode ray tube directly, in the normal way, with both eyes.

Finally, the television presentation makes it very easy to adjust tube brightness and amplifier gain, in order to obtain the best picture quality.

These advantages of the television approach must of course be weighed against the accompanying deterioration in modulation transfer resulting from the addition of a camera tube, and the increase in size, weight, bulk and cost of the equipment.

5.2. *The problems of the scanning mechanism*

Three different ways of reading out the charge image from the storage target in a camera tube have been considered for application under starlight illumination. These are the vidicon, the orthicon and the isocon mode of operation.

All three are based on the principle of cathode-potential stabilization, where a positive charge image corresponding to the optical image, is built up on the storage target.

The scanning electron beam removes the charge during a frame scan from each element in succession by approaching the target with such a low velocity that the secondary emission coefficient is smaller than unity. Negative charge is thus deposited, and the potential of the target element drops until it practically reaches that of the cathode of the electron gun. From then on no further electrons can reach the element, which is thus stabilized at cathode potential.

As a result of the velocity spread in the electrons emitted from the hot cathode of the electron gun, the stabilizing action becomes less effective as the potential of the scanned element drops, and can never be entirely completed. This can easily give rise to annoying picture lag if the total amount of charge corresponding to the picture brightness, is not sufficiently large. A smaller target capacitance improves this situation by leading to a higher potential excursion for

the same amount of picture charge and thus to a more effective removal by the scanning beam. This may, however, lead to a much smaller dynamic range of the pick-up tube because the total potential excursion on the target is usually restricted by other factors. The performance of the tube at higher levels of illumination suffers as a result, thus limiting the optimum signal-to-noise ratio in the video signal.

The second problem, created by an insufficiently large amount of picture charge, is that of excessive electrical noise in the video signal.

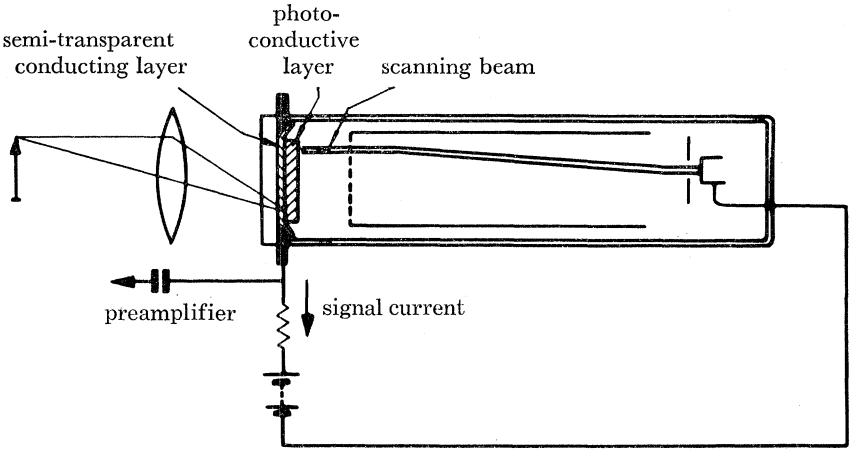

FIGURE 23. Schematic diagram of a vidicon.

The simplest method of reading out the video signal while removing the picture charge by the scanning beam is that employed with the vidicon, as illustrated in figure 23. The conductive signal plate on the side of the storage target opposite to that scanned by the beam is coupled directly into the video amplifier. This provides the best solution from the point of view of compactness and ease of operation, and is now the mode of operation generally preferred in television broadcasting and industrial applications.

If the amount of picture charge is very small however, it can lead to the fixed amplifier noise becoming the limiting component in the signal : noise factor of the video signal. This situation can only be avoided for starlight viewing applications, if the optical image is sufficiently intensified before the charge image is formed.

The orthicon mode of operation (Rose, Weimer & Law 1946) avoids the noise contributions of the video amplifier by multiplying the electrons of the returning scanning beam in a secondary electron multiplier. These electrons are reflected by the target because their energy is insufficient to reach and neutralize the remaining positive picture charge. The result is a different noise contribution by the camera tube itself, resulting from the statistical fluctuations in the number of electrons in the returning beam. The largest noise contribution corresponds in this case to the darker areas in the picture, where more electrons return.

This problem is minimized in the isocon scanning mode (Weimer 1949). As long as a positive charge is present on the target, some of the electrons in the scanning beam are affected by the resulting fields near the target, and are returned with a modified lateral velocity component. These 'scattered' electrons can be separated from the normally reflected electrons, and steered towards the secondary electron multiplier.

The resulting beam noise can be lower than in the orthicon scanning mode, and the highest

noise now corresponds correctly to the highlights in the scene. Optimum operation of the tube requires careful adjustment and control of the various magnetic and electrostatic fields to obtain correct separation of the appropriate electrons in the scanning beam.

The image orthicon and image isocon pick-up tubes combine the indicated modes of scanning with an electron-optical image section to convert the optical image into the charge pattern. This section contains a photo-emissive cathode, an electron-optical lens and the storage target. These image sections, added to the space required for the more complicated scanning mechanism, lead to larger tube envelopes than is normal in a camera tube of the vidicon type, with a comparable modulation transfer function. On the other hand, they can operate satisfactorily at much lower brightness levels of the input image than can the vidicon.

5.3. *The main parameters*

Three important parameters characterize the performance of a low light level television chain.

The first of these is the signal : noise ratio in the video signal as a function of the mean illumination on the photocathode. In a high-quality camera chain for television broadcasting, this ratio can be above 400 for normal studio broadcasting, when employing 625 lines and 50 interlaced frames per second.

For a particular scene, such as a black and white bar pattern, it has been shown in §2.2 that a minimum signal : noise ratio of about 1 is required for detection, provided that the noise is due to the random fluctuations in the numbers of detected photons, which can be integrated over the bar width. In that situation it is therefore possible to express the noise limitation in terms of the limiting resolution in black and white bars per picture width, as a function of the photocathode illumination.

In the television case the picture is formed with a fixed number of scanning lines and the noise performance of the television camera chain is normally expressed as a peak-signal current: r.m.s. noise current ratio. The value of this ratio depends on the number of scanning lines, determining the required bandwidth of the video signal, while the signal amplitude for a black and white bar pattern depends on the width of the bars and the mean photocathode illumination.

It is thus possible to relate the limiting number of black and white bars which can just be resolved, i.e. the 'resolution lines' n_{lim}, to the signal current:r.m.s. noise current ratio and bandwidth of the video signal.

This procedure has been described in §5.4 and can yield acuity curves of low light level television chains, which express their noise-resolution performance in terms of the limiting number of 'lines' still resolvable in the image of a black and white bar pattern, as a function of the mean illumination level I_{m} of the primary photocathode. Reference to the parameters of the selected objective lens enables the conversion of n_{lim} and I_{m} into the angular size α and luminance L_{m} of the object in the scene.

The overall m.t.f. of the composite camera tube, in this case expressed as its 'square-wave' response, $R(n)_{\mathrm{sq}}$, is the second important parameter for its resolution performance. This can also be indicated as the relative response (in uncorrected signal amplitude) as a function of the spatial resolution in 'lines' per picture width.

This square-wave response can again be combined with the noise–resolution performance, in order to produce overall acuity curves, which are similar to those for direct viewing instruments indicated in figure 1.

The third important characteristic is the performance of the camera chain when observing moving objects. A suitable way of indicating the effect is to compare the static limiting resolution with the dynamic one, obtained when the picture is moved across the photocathode at a constant velocity of, for example, one complete picture width every 10 or 20 s. This provides a good comparison of different approaches with regard to picture lag.

5.4. *The acuity curves*

The noise performance of a television camera chain is normally expressed as the peak signal current: r.m.s. noise current ratio in the video signal. The noise current results in this case from the combination of the various noise components in the chain, when these are added in quadrature.

When photoelectron multiplication of one kind or another has taken place before the formation of the charge image, the peak signal current in the camera tube will be equal to the signal component of the photocurrent, multiplied by the various processes of electron multiplication employed.

Provided that each of these processes has fluctuations of a Gaussian nature, the mean square value of these fluctuations can be expressed as

$$\overline{\Delta i^2} = 2e\bar{i}F(1+\sigma_n+\sigma_n\sigma_{n-1}+\ldots+\sigma_n\sigma_{n-1}\ldots\sigma_1),$$

where $\bar{i}$ is the mean current (A), e is the electron charge ($= 1.6\times10^{-19}$ C), F is the bandwidth (Hz) and σ_1, σ_2, ... are the average numerical factors in the multiplication processes.

Any other noise currents, such as, for instance, the equivalent noise current of the video amplifier in the case of the vidicon, or the noise in the returning scanning beam of an orthicon or isocon, must be added to the photon-noise current in quadrature.

The resulting peak signal-current to r.m.s. noise-current ratio, taking into account a picture aspect ratio of 3:4, and 25 % raster blanking, will be

$$S/N = \frac{2\times10^{-4}\eta I_m C w^2\sigma_n\sigma_{n-1}\ldots\sigma_1}{[2eF.10^{-4}\eta I_m w^2\sigma_n\sigma_{n-1}\ldots\sigma_1(1+\sigma_n+\sigma_n\sigma_{n-1}+\ldots\sigma_n\sigma_{n-1}\ldots\sigma_1)+\sum_m(\bar{i}_{\text{noise}})^2_m]^{\frac{1}{2}}}.$$

If $\sigma_n\,\sigma_{n-1}\ldots\sigma_1$ is replaced by G_0, and σ_1 is sufficiently large, this can also be written as

$$S/N = \frac{2\times10^{-4}\eta I_m C w^2 G_0}{[2eF.10^{-4}\eta I_m w^2 G_0^2+\sum_m(\bar{i}_{\text{noise}})^2_m]^{\frac{1}{2}}}, \tag{4}$$

where I_m is the mean photocathode illumination $= \frac{1}{2}(I_{\text{high}}+I_{\text{low}})$ (lx), η is the photocathode sensitivity (Alm^{-1}), C is the contrast $= (I_{\text{high}}-I_{\text{low}})/(I_{\text{high}}+I_{\text{low}})$, w is the picture width on photocathode (cm), G_0 is the total average electron gain from primary photoelectron to electronic charge on the storage target, e is the electron charge (1.6×10^{-19} C), F is the bandwidth (Hz) and $(\bar{i}_{\text{noise}})_m$ is the mean noise current of mth noise component.

The expression for the signal:noise ratio in the video signal of equation (4) can now be related to the limiting resolution expressed as the number of lines per picture width, in the following way.

In the case of a test object consisting of a black and white bar pattern the peak signal current: r.m.s. noise current ratio of equation (4) for the purely photon-noise limited situation can be written as

$$(S/N)_{\text{video}} = \frac{2\times10^{-4}(I_m\eta)^{\frac{1}{2}}Cw}{(2\times10^{-4}eF)^{\frac{1}{2}}} = 3.54\times10^7\left(\frac{I_m\eta}{F}\right)^{\frac{1}{2}}Cw. \tag{5}$$

PHILOSOPHICAL TRANSACTIONS OF THE ROYAL SOCIETY A MATHEMATICAL, PHYSICAL & ENGINEERING SCIENCES

The same black and white bar pattern leads, according to equation (1) to a signal:noise ratio in the photons received by two adjacent elements on the photocathode of

$$(S/N)_{\text{photons}} = \frac{(L_m \tau \theta P)^{\frac{1}{2}} \alpha C D}{(7.5 \times 10^{10})^{\frac{1}{2}}}. \tag{6}$$

Substituting in equation (6):

$$L_m = I_m 4(f_0/D)^2 1/\pi; \theta P = 6.28 \times 10^{18} \eta,$$

and

$$\alpha = 57.3 \times 60 \times \frac{w}{n_{\text{lim}} f_0},$$

where n_{lim} = the maximum number of black and white bars just discernible per picture width, leads to

$$(S/N)_{\text{photons}} = \frac{3.54 \times 10^7 C w (I_m \tau \eta)^{\frac{1}{2}}}{n_{\text{lim}}}.$$

Since the minimum signal:noise ratio in the registered photons, required for detection of a black and white bar pattern is approximately 1, this expression can also be written as

$$n_{\text{lim}} = 3.54 \times 10^7 (I_m \tau \eta)^{\frac{1}{2}} C w \tag{7}$$

which, combined with equation (5) for the signal:noise ratio in the video signal leads to the simple approximation

$$n_{\text{lim}} \simeq (F\tau)^{\frac{1}{2}} (S/N)_{\text{video}}. \tag{8}$$

This is a general expression for the limiting resolution of a black and white bar pattern in television pictures, for the case of 'white' noise, a bandwidth of F Hz and an integration time of the system equal to τ seconds.

On the basis of similarity considerations, Coltman & Anderson (1960) derived the same expression with an undefined constant: $n_{\text{lim}} = \text{constant} \times F^{\frac{1}{2}} \times (S/N)$. They determined the value of the constant experimentally as 1.23 for a sinusoidal bar pattern and with (S/N) measured as the ratio of r.m.s. signal:r.m.s. noise (their equation quotes line-pairs and a constant 0.615).

The peak signal is $\sqrt{8}$ times as large as the r.m.s. signal for a sine wave. The experimentally determined constant in Coltman & Anderson's equation must therefore be reduced by $\sqrt{8}$ for a sine wave bar pattern, if (S/N) is expressed as peak signal:r.m.s. noise ratio, bringing it very close to that of equation (8) for an integration time of about 0.2 s.

The effect of picture degradation as a result of the modulation transfer in the camera chain can be accounted for by replacing the contrast C in equation (4) by the product of the input contrast C_i and the square wave response $R(n)_{\text{sq}}$ of the combined intensifier-camera tube.

Any reduction in picture resolution due to modulation transfer will be accompanied by a corresponding reduction in the perceptibility of that part of the noise which was present before the picture degradation took place. The highest noise frequencies are increasingly attenuated and the photon noise will no longer be 'white'. This can be accounted for by taking for the value of F in the photon-noise term the resulting 'effective' bandwidth as reduced by the modulation transfer, instead of the full bandwidth of the video amplifier. (See Appendix.)

Assuming that equation (8) has general validity and will still hold approximately if the noise is not 'white', (S/N) can be eliminated from equation (4), leading to

$$I_m = \frac{4 \times 10^{-16} n^2}{\eta C_i^2 w^2 \tau R(n)_{\text{sq}}^2} \left[1 + \sqrt{\left\{ 1 + \frac{1.56 \times 10^{38} C_i^2 \tau R(n)_{\text{sq}}^2 \sum_m (\bar{i}_{\text{noise}})_m^2}{F_{\text{eff}} G_0^2 n^2} \right\}} \right]. \tag{9}$$

This is a general expression for the acuity curve of a low light level television camera chain. A similar equation has been derived by Rosell (1969), with a somewhat different analysis, leading to slightly different constants.

The various mean noise current terms in equation (9) can be evaluated more closely for the different scanning mechanisms.

In the case of vidicon read-out, the amplifier terms are important. These are:

(*a*) The noise contributed by the signal R_S:

$$(\bar{\imath}_n)^2_{R_S} = \frac{4kTF}{R_S}.$$

(*b*) The noise contributed by the first amplifier valve (or an equivalent expression if a solid-state amplifier is used):

$$(\bar{\imath}_n)^2_v = \frac{4kTFR_{eq}}{R_S^2}(1+\tfrac{4}{3}\pi^2F^2R_S^2C_p^2), \tag{10}$$

where k is Boltzmann's constant $= 1.38\times10^{-23}JK^{-1}$, T is the absolute temperature (K), F is the bandwidth (Hz), R_{eq} is the equivalent noise resistance of the valve and C_p is the parasitic capacitance from camera tube output to earth.

The term $1+\frac{4}{3}\pi^2F^2R_S^2C_p^2C_p^2$ is caused by the necessity to amplify the higher frequencies more, in order to compensate for the effectively lower signal resistor resulting from the parasitic capacitance C_p, which is parallel to R_S.

In practice the noise resulting from the nonlinear amplification of different frequencies gives rise to a sharp increase in the noise at higher frequencies which, for the same numerical value of signal to r.m.s. noise, makes this noise much less objectionable.

For orthicon read-out the significant noise is the shot noise in the return beam. This noise current is proportional to the signal current, and must be at least a factor 2 to 2.5 larger in order to discharge the target sufficiently well in one scanning operation.

The signal:noise ratio of the orthicon (and isocon) is somewhat further decreased by the multiplier noise, but in practice this has been found to be less than about 7 %.

In the isocon mode the shot noise in the scattered return beam will be even smaller, due to the higher modulation depth obtainable, and will be almost absent in the dark areas.

Equation (9), with C replaced by $C_iR(n)_{sq}$ and with the appropriate additional noise currents $(\bar{\imath}_{noise})_m$ evaluated, can now be used to compare the thus predicted performance of any particular low light-level camera chain with the measured values.

Two examples have been considered. The first of these is a system comprising three cascaded image intensifier modules with 25 mm photocathode ($w = 2$ cm), coupled optically into a plumbicon. Measurements on this combination have been reported by Taylor, Petley & Freeman (1969).

The parameters of equation (8) were in their case:

$$\eta = 1.7\times10^{-4}, \qquad F_{eff} = 5\times10^5\ \text{Hz},$$
$$C = 1, \qquad G_0 = 3\times10^4\ \text{(estimated)},$$
$$w = 2\ \text{cm}, \qquad (\bar{\imath}_{noise})_{amplifier} = 1.6\times10^{-9}\ \text{A}.$$

Figure 24 shows the computed acuity curve for an assumed integration time of 2 frames: $\tau = 0.08$ s, together with the measured points.

It appears that the performance of this camera tube combination is almost entirely photon-noise limited, but the overall optical performance of the comparatively large number of cascaded components forms the main resolution limitation for smaller objects.

For this reason approaches with fewer components would be preferred.

An alternative arrangement can, for instance, be provided by coupling two intensifier modules to a plumbicon with a fibre-optic input window. This, however, is a more expensive solution as it requires a non-standard camera tube. The brightness gain will also be lower, and the photon noise is no longer the only noise limitation. The overall m.t.f., on the other hand, should be improved and a better performance obtainable at higher photocathode illumination levels.

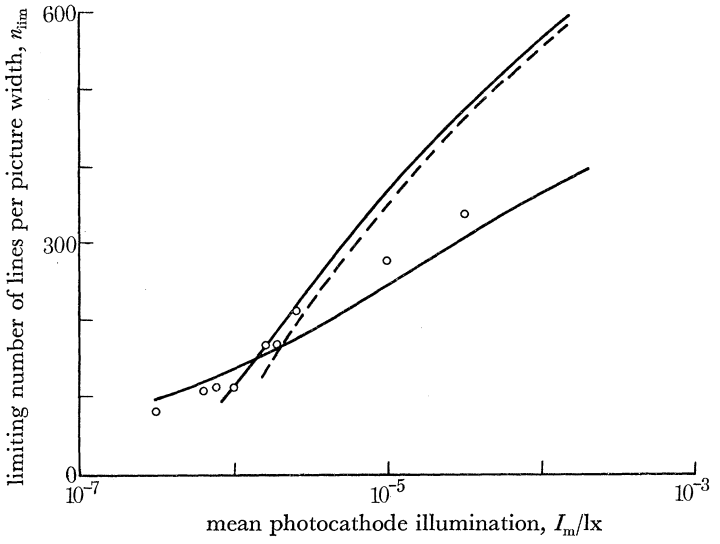

FIGURE 24. Computed and measured acuity curves. Three fibre-optic modules (XX 1060) + standard plumbicon (—, calculated; ○, measured). I.s.e.c. tube WL-32000 (—, calculated; – – –, published data).

The optical performance can be improved still further by building one of the intensifier stages directly into the camera tube, as in the so-called secondary-electron-conduction vidicon. In this tube (Goetze & Boerio 1964) an electron-optical image stage precedes the storage of the image on the target, which is similar to the thin films in a through-secondary-electron-multiplier image tube, described in §3.3.

The unfavourable noise performance of the s.e.c. vidicon, employed on its own, can be greatly improved by coupling the tube fibre-optically to one further image intensifier module. This combination is called the intensifier s.e.c. vidicon, or i.s.e.c. tube, and has been used as the second example of employing equation (9) for calculating acuity curves.

The specific example is the Westinghouse WL-32000, using an intensifier module with 40 mm photocathode and 25 mm screen size, fibre-optically coupled to a s.e.c. vidicon.

Taking into account the published square-wave response of this i.s.e.c.–tube combination, suitably converted to lines per picture width, and with its other parameters as published:

$$\eta = 2.25 \times 10^{-4}\,\mathrm{A\,lm^{-1}}, \qquad (\bar{\imath}_{\mathrm{noise}})_{\mathrm{amplifier}} = 3 \times 10^{-9}\,\mathrm{A}$$
$$F_{\mathrm{eff}} = 10^{6}\,\mathrm{Hz} \qquad G_0 = 2 \times 10^{3},$$

figure 24 shows its calculated acuity curve in comparison with the published one for 100% contrast, and again an assumed integration of 0.08 s. The measured curve in figure 24 has also been converted to lines per picture width and mean photocathode illumination.

The agreement between the computed and the measured performance appears again to be very good.

Despite its larger photocathode, this i.s.e.c. tube has not such a good performance at the lowest light levels as the plumbicon-cascaded stack combination. For objects with a high contrast and an image size requiring a resolution of more than about 150 lines per picture width on the photocathode, the i.s.e.c. tube begins to gain. The reason for this is that the i.s.e.c. tube is at starlight illumination levels still mainly limited by amplifier noise, and only for a photocathode illumination above 10^{-5} lx does the photon noise current begin to overtake the amplifier noise.

It is claimed that the performance of an intensifier-image orthicon is very similar to that of an i.s.e.c. tube with equal size photocathode, and for a static image.

No similar performance data appear to be available at present for the combination of an image intensifier with an image isocon, but the improvement of isocon scan over orthicon scan decreases as the image is intensified in an additional intensifier module, and disappears completely when the instrument becomes photon-noise limited.

5.5. *Conclusions and future possibilities*

When comparing some of the low light level television systems discussed, it is clear that a simple and cheap solution can at present be provided by coupling a stack of fibre-optic image intensifier modules optically into a standard vidicon or plumbicon camera tube. Such a system can not only provide a performance, which is limited by photon-noise at starlight illumination levels, but is also very easy to operate and needs no complicated adjustment procedures.

The disadvantage of this approach is the optical resolution limitation at somewhat higher light levels, caused by the cumulative effect of the modulation transfer in a comparatively large number of separate components.

This can be somewhat improved by coupling two modules directly into a vidicon or plumbicon with fibre-optic input window. However such a camera tube is more expensive and, as a result of the lower initial brightness gain, is no longer completely photon-noise limited.

An even better optical performance can be obtained with tube combinations of the i.s.e.c. vidicon and of the intensifier-image orthicon and isocon type. These solutions require more carefully controlled adjustments in order to obtain the best picture quality.

As a result of its lower initial electron gain, the i.s.e.c. vidicon is still mainly limited by video amplifier noise under starlight conditions. The storage target in this tube is not very robust and can easily be damaged, either by mechanical shock or by burn-in when observing high-lights in the scene.

The intensifier image orthicon and isocon, with their even lower initial electron gain of no more than about a factor 100, must operate with a much smaller amount of charge on the storage target. This can give rise to serious lag in moving pictures under starlight conditions. This lag can only be made acceptable by reducing the target capacitance drastically. In turn, this will reduce the operating range of the tubes and result in a limited optimum signal: noise ratio when the light level is increased.

A recently announced new approach to low light-level television is the integral silicon intensifier camera tube, illustrated in figure 25. This tube is basically like a vidicon with a thin single crystal silicon target, about 10 to 15 μm thick. The target contains a very large number of small p–n junctions on its surface scanned by the electron beam, operating in the vidicon mode.

PHILOSOPHICAL TRANSACTIONS OF THE ROYAL SOCIETY A MATHEMATICAL, PHYSICAL & ENGINEERING SCIENCES

The other side of the target is bombarded by the photoelectrons of the integral image section. These photoelectrons strike the silicon target with an energy of about 10 keV and produce a few thousand charge carriers, which diffuse through the p–n junctions to the other side of the target, where their charge can be removed by the scanning beam.

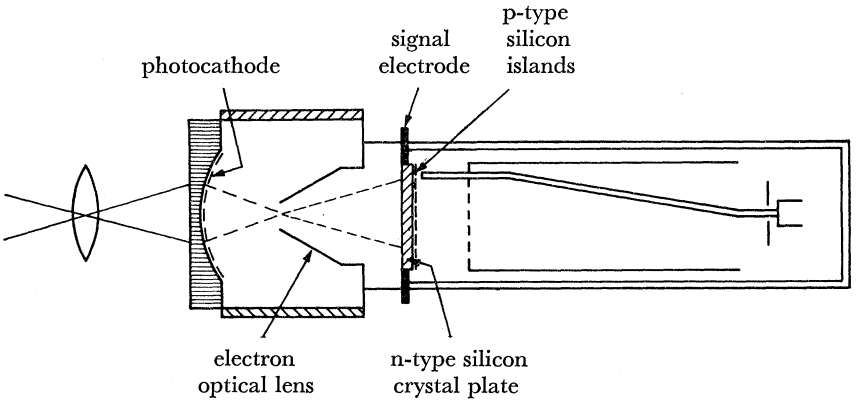

FIGURE 25. Illustration of the principle of operation of an integral silicon-intensifier-camera-tube.

Tubes of this type are still in the experimental stage, and need considerable further development before blemish-free targets can be produced and the picture quality equals that of present vidicon or plumbicon tubes. Nevertheless, this appears to be a very interesting development, which could lead to a much more robust and satisfactory approach than the i.s.e.c. tube.

If required, a further stage of image intensification could also be added to this tube via a fibre-optic input window.

A satisfactory solution in the nearer future could possibly be the combination of a high-quality channel image intensifier tube, as discussed in §3.4, with a vidicon or plumbicon. The potentially much better modulation transfer function of the channel tube in comparison with the cascaded stack, could make this a very attractive proposition. It may combine low cost and ease of operation with a good optical performance, while avoiding amplifier noise limitations.

APPENDIX. CALCULATION OF EFFECTIVE BANDWIDTH

An estimate of the 'effective bandwidth' can be obtained as follows. The sine wave response curve appears to resemble in general a curve of the shape $1/[1+(n/n_0)^2]$, where n_0 is the number of lines per picture width at which the modulation depth has fallen to 50 %. Taking into account an overall blanking time of about 25 % and an aspect ratio of 4:3, it is possible to define an effective bandwidth as

$$F_{\text{eff}} = \frac{N_{\text{eff}}^2}{2\tau_0}, \quad \text{where} \quad N_{\text{eff}} = \int_{n=0}^{N_0} \frac{\mathrm{d}n}{1+(n/n_0)^2},$$

if $0.75N_0$ = number of scanning lines, and τ_0 = frame time.

This leads to

$$F_{\text{eff}} = \frac{n_0^2[\tan^{-1}(N_0/n_0)]^2}{2\tau_0}.$$

If only the square wave response is obtainable, n_0 can be found from that curve as the value of n where $R(n)_{\text{sq}}$ has fallen to about 60 %.

References

Adams, J. & Manley, B. W. 1965 *Electron. Engng* **37**, 180.
Bathelemy, R. & Zeitline, V. 1936 French Patent 802244.
Blackwell, H. R. 1946 *J. opt. Soc. Am.* **36**, 624.
Campbell, F. W. 1968 *Proc. I.E.E.E.* **56**, 1009.
Coltman, J. W. 1954 *J. opt. Soc. Am.* **44**, 468.
Coltman, J. W. & Anderson, A. E. 1960 *Proc. I.R.E.* **48**, 858.
Emberson, D. L. & Long, B. E. 1969 *Adv. Electronics Electron Phys.* **28**A, 119.
Farnsworth, P. T. 1930 U.S. Patent no. 1969399.
Goetze, G. W. & Boerio, A. H. 1964 *Proc. I.E.E.E.* **52**, 1007.
Goodrich, G. W. & Wiley, W. C. 1962 *Rev. scient. Instrum.* **33**, 761.
Gubisch, R. W. 1967 *J. opt. Soc. Am.* **57**, 407.
Jones, R. C. 1959 *J. opt. Soc. Am.* **49**, 645.
Krisek, V. & Vand, V. 1946 *Electron. Engng* **18**, 316.
Kühl, W., Geurts, A. & Overhagen, J. V. 1969 *Adv. Electronics Electron Phys.* **28**B, 615.
Manley, B. M., Guest, A., & Holmshaw, R. T. 1969 *Adv. Electronics Electron Phys.* **28**A, 471.
Oshchepkov, P. K., Skvortsov, B. N., Osanov, B. A. & Siprikov, I. V. 1960 *Pribory Tekh. Eksp.* **4**, 89.
Pirenne, M. H., Marriott, F. H. C. & O'Doherty, E. F. 1957 *Spec. Rep. Ser. med. Res. Coun.* no. 294.
Richards, E. A. 1969 *Adv. Electronics Electron Phys.* **28**B, 661.
Rose, A. 1942 *Proc. I.R.E.* **30**, 295.
Rose, A., Weimer, P. K. & Law, H. B. 1946 *Proc. I.R.E.* **34**, 424.
Rosell, F. A. 1969 *J. opt. Soc. Am.* **59**, 539.
Schade, O. H. 1948 *R.C.A. Rev.* **9**, 653.
Schade, O. H. 1956 *J. opt. Soc. Am.* **46**, 721.
Schagen, P., Bruining, H. & Francken, J. C. 1952 *Phillips Res. Rep.* **7**, 119.
Schagen, P. & Turnbull, A. A. 1969 *Adv. Electronics Electron Phys.* **28**A, 393.
Stark, A. M., Lamport, D. L. & Woodhead, A. W. 1969 *Adv. Electronics Electron Phys.* **28**B, 567.
Sternglass, E. J. 1955 *Rev. scient. Instrum.* **26**, 1202.
Taylor, D. G., Petley, C. H. & Freeman, K. G. 1969 *Adv. Electronics Electron Phys.* **28**B, 837.
de Vries, H. 1943 *Physica* **10**, 553.
Walsh, J. W. T. 1958 *Photometry*, p. 55. London: Constable and Co.
Weimer, P. K. 1949 *R.C.A. Rev.* **10**, 366.
Woodhead, A. W., Taylor, D. G. & Schagen, P. 1963/64 *Philips Tech. Rev.* **25**, 88.

PHILOSOPHICAL TRANSACTIONS OF THE ROYAL SOCIETY A MATHEMATICAL, PHYSICAL & ENGINEERING SCIENCES

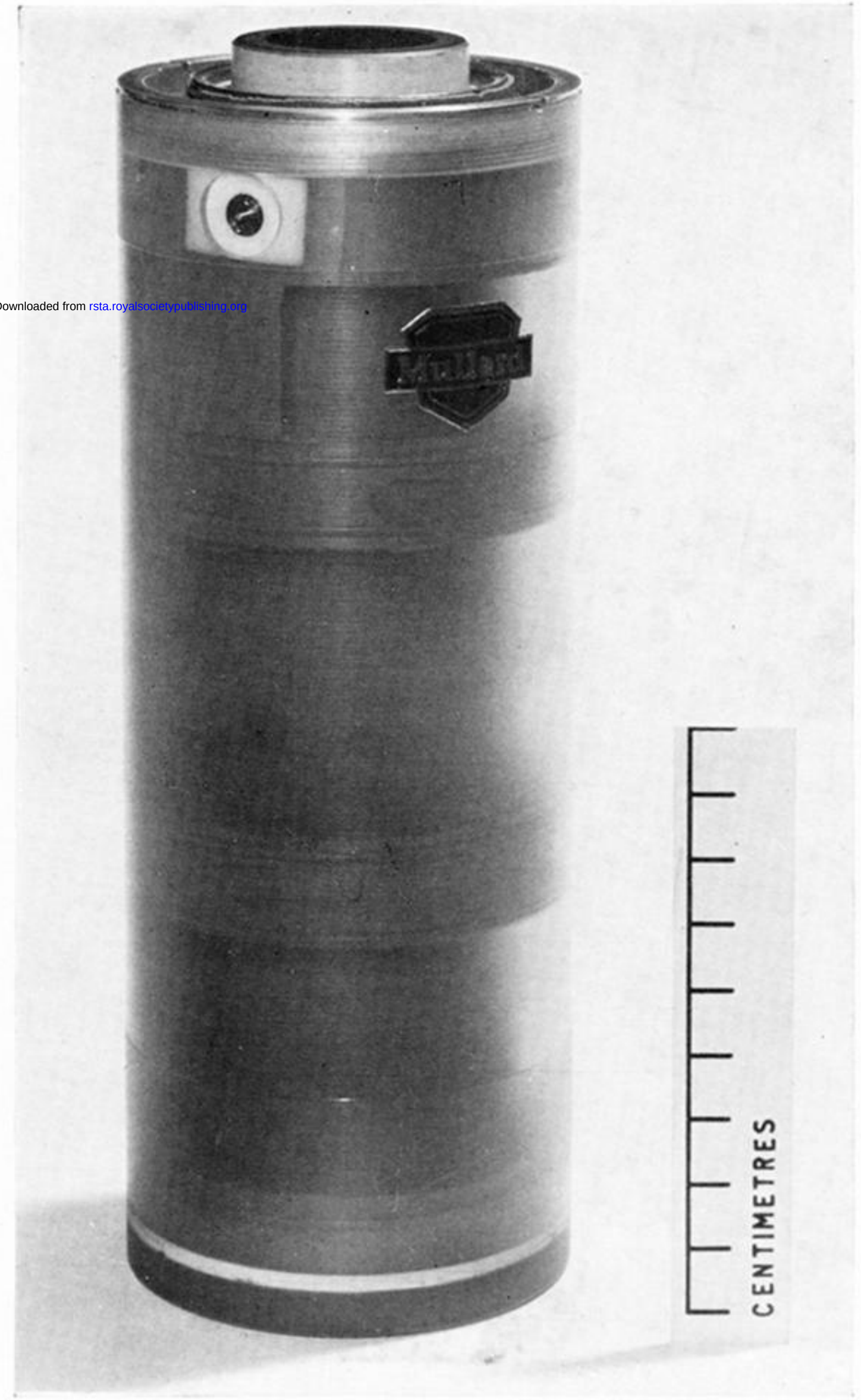

IGURE 16. Photograph of stack of three image tube molecules with fibre-optic coupling and integral power supply unit (XX 1060).

FIGURE 22. Photograph of the image on the viewing screen of an experimental channel image intensifier tube.

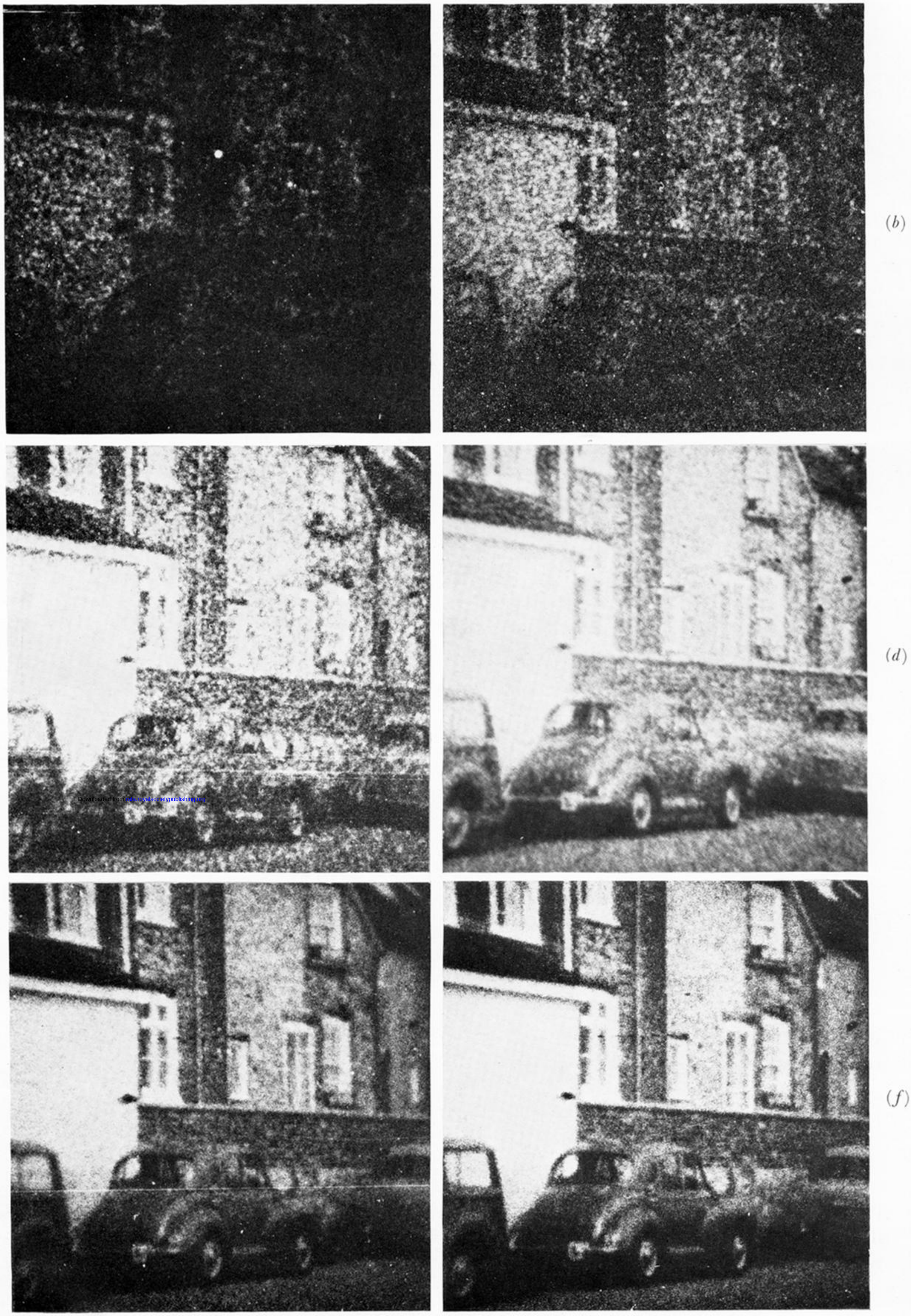

FIGURE 18. Photograph of image detail on screen of XX 1060, corresponding to different scene illumination levels, with an exposure time of 0.2 s. (*a*) 0.03 mlx (very dark sky, no moon), (*b*) 0.1 mlx, (*c*) 0.3 mlx, (*d*) 1 mlx (approx. starlight: no cloud, no moon), (*e*) 2 mlx, (*f*) 50 mlx (approx. full moon).